June, 1980

InGaAsP QUATERNARY MATERIALS FOR NEAR INFRARED DETECTOR AND LASER APPLICATIONS

Final Report

for period 01-01-77 through 02-29-80

Contract No. N00014-77-C0086

General Order No. 3316

Project No. 7D10

Department of Electrical Engineering

University of Illinois at Urbana-Champaign

Urbana, Illinois 61801

Sponsored by

Advanced Research Projects Agency (DOD)

ARPA Order No. 3316

Monitored by Office of Naval Research Under

Contract No. N00014-77-C0086

Nick Holonyak Jr.
N. Holonyak, Jr.,

G.E. Stillman
G.E. Stillman

Principal Investigators

(12) 64

(11) Jun[redacted]980

(6) InGaAsP QUATERNARY MATERIALS FOR NEAR INFRARED DETECTOR AND LASER APPLICATIONS.

(9) Final Report. 1 Jan 77-29 Feb 80

for period 01-01-77 through 02-29-80

(15) Contract No. N00014-77-C0086, NARPA Order-3316

General Order No. 3316

Project No. 7D10

Department of Electrical Engineering

University of Illinois at Urbana-Champaign

Urbana, Illinois 61801

(10) N. Holonyak, Jr. G. E. Stillman

Sponsored by

Advanced Research Projects Agency (DOD)

ARPA Order No. 3316

Monitored by Office of Naval Research Under

Contract No. N00014-77-C0086

Nick Holonyak Jr.

N. Holonyak, Jr.,

G. E. Stillman

G.E. Stillman

Principal Investigators

TABLE OF CONTENTS

I. INTRODUCTION

In recent years the quaternary system $In_{1-x}Ga_xP_{1-z}As_z$ has drawn much attention because, when grown lattice-matched on InP, it extends from λ~0.92 to 1.68 μm as a laser source or as a detector. In this wavelength range fiber optic transmission is optimum, and is, of course, the reason for much of the unusual interest in InGaPAs. In this project we have been concerned with the liquid phase epitaxial (LPE) and vapor phase epitaxial (VPE) growth of this quaternary system. A number of the basic features of the LPE growth of InGaPAs on InP have been identified. InP-$In_{1-x}Ga_xP_{1-z}As_z$ heterostructure lasers and detectors have been constructed and have been studied. These results are described below.

II. QUATERNARY QUANTUM-WELL HETEROSTRUCTURES

One portion of this work has been concerned with quantum-well InP-$In_{1-x}Ga_xP_{1-z}As_z$ lasers. The history of this work is described in some detail in Ref.1 and will not be repeated here. Perhaps the simplest form of quantum-well laser is a conventional double heterojunction in which the active region has been shrunk in width to well below L_z~500 Å, i.e., into the range where the de Broglie wavelength of light-mass electrons (or that of the light-mass holes) is of the order of the active region size or width, L_z. Then the carriers must exhibit the confined-particle behavior reminiscent of the well-known problem of a particle in a finite potential square well. For such case, the usual allowed states at the band edge are cut-off, and a subband of states (of constant density) appears at the position of the first confined-particle state of the heterostructure square well, a second subband of states appears at the second state, etc. This behavior applies to electrons in the conduction band, and similarly to holes in the valence band. In any event,

the usual parabolic band edge of a bulk semiconductor is cut-off and, in effect, is raised and modified into a well-defined step. This immediately defines a new form of semiconductor laser. To achieve a sufficient active region volume it is only necessary to couple together several quantum wells. Even for 50 Å coupling barriers this does not lead to very much broadening of the lowest confined-particle states of a multiple-quantum-well heterostructure.

Although the most elementary form of quantum-well laser is simply an ordinary double heterojunction (DH) with an unusually thin active region (L_z<500 Å), the first quantum-well laser diode was constructed in the InP-InGaPAs system with a multiple active region. This work is reported in Ref. 2. (The work on Refs. 2-12 received primary support from this contract; these references provide a detailed description of quaternary quantum-well heterostructure lasers.) It is worthwhile to note that Ref. 2 describes: 1) the first quantum-well injection laser, 2) the first quantum-well heterostructure grown successfully by LPE, and 3) the first quaternary (InGaPAs) quantum-well heterostructure. Because the coupling barriers of the multiple quantum-well laser diodes of Ref. 2 are relatively thick, these diodes operate essentially as single quantum-well heterostructures. Accordingly, and to simplify the study of quantum-well lasers, we have examined a number of single-quantum well InP-$In_{1-x}Ga_xP_{1-z}As_z$ heterostructures. These heterostructures exhibit unusual bandfilling properties, and laser operation over a remarkable spectral range (Refs. 3, 5, 6). The quantum-well confined-particle transitions are clearly revealed in this form of laser operation. Also, these data, along with those on MO-CVD $Al_xGa_{1-x}As$-GaAs described in Ref. 1, show for the first time that band-to-band recombination in a semiconductor

can be observed from high (in energy) above the conduction and valence band edges. In other words, now it is known, based on this and related work (see Ref.1), that carriers within a band--not just at the band edges--can be manipulated and can participate in radiative recombination.

Another distinctive property of quantum-well heterostructure diodes is that carrier injection, with radiative recombination, can occur via tunneling. The first observation of these effects is described in Ref.4. An even more striking example is shown in Fig.22 of Ref.1. In other words, we have shown unambiguously that carriers can be "injected" by tunneling. This could become important in the circumstance where it is desired that "injected" carriers not enter the active region "hot", as they do, in fact, in the case of conventional DH lasers.

Ordinarily the carriers introduced by photopumping or by injection (current) into a quantum-well active region are "hot". If only one or two small quantum wells make up the active region (InGaPAs), then electrons, being light in mass and traveling a considerable distance before scattering, can travel right across an InGaPAs quantum well. That is, they remain "hot" compared to the states within the quaternary quantum well. On the other hand, heavy holes travel only a small distance before scattering, and can be collected in a quaternary quantum well. Then "hot"-electron recombination with a bound hole, a collected hole, occurs at an energy $E_g(InP)-\Delta E_v$, where ΔE_v is the valence band discontinuity between InP and InGaPAs. Since $E_g(InP)$ and $E_g(InGaPAs)$ are known and thus $\Delta E_g \equiv E_g(InP)-E_g(InGaPAs)=\Delta E_c+\Delta E_v$, ΔE_c can be determined immediately. This measurement, which is described in Ref.7, has for the first time provided the experimental value $\Delta E_c \simeq 2E_v$. (This measurement contradicts a previous theoretical result maintaining that $\Delta E_v > \Delta E_c$. See the references in Ref.7.)

In related work on MO-CVD $Al_xGa_{1-x}As$-GaAs heterostructures (Ref.1), we have discovered that, because of the quasi-two-dimensional form of a quantum-well active region, phonon participation in the carrier recombination (unlike in bulk crystal) is an important process, and laser operation on phonon sidebands can be observed $\hbar\omega_{LO}$, or even $2x\hbar\omega_{LO}$, below the lowest confined-particle transitions. Observations of the same type on quantum-well InP-$In_{1-x}Ga_xP_{1-z}As_z$ heterostructures are reported in Ref.8. We note that in all of these heterostructures the active regions are small (very compact), and as the excess carriers ("hot" carriers) thermalize in the quantum-well phonons are generated and may even be stimulated. A rather complete discussion of these effects is given in Ref.9, which is probably the most complete published account that now exists on quantum-well InP-$In_{1-x}Ga_xP_{1-z}As_z$ heterostructure lasers.

Various practical features are expected and have emerged from this work on quantum-well heterostructure lasers. One of these is the fact that this form of laser is less temperature sensitive than conventional double heterojunctions. Thus far MO-CVD $Al_xGa_{1-x}As$-GaAs quantum-well heterostructures have exhibited the lowest temperature sensitivity, with T_o as high as 437°C in the threshold expression $J_{th}(T) = J_0\exp(T/T_o)$. The results for InP-$In_{1-x}Ga_xP_{1-z}As_z$ are not as good but, nevertheless, are much better than for conventional quaternary heterostructure lasers. This is an important result and is described in Ref.10.

Although it has not been mentioned yet, when our work on InP-$In_{1-x}Ga_xP_{1-z}As_z$ quantum-well heterostructure lasers began (1977), the LPE crystal growth crucible, a cylindrical boat, was driven (operated) manually. This apparatus (see Ref.9) has been mechanized, outfitted with a stepper motor, and is now controlled with a small computer. As the crystal cross sections of Ref.9

show (Figs.4, 5, 6), we are able to grow 10 or more uniform InGaPAs quantum-well layers of size as small as L_z~100 Å. We have demonstrated unequivocally that LPE, and not just MBE, is a viable method to grow quantum-well heterostructures. One further major development has occurred in this work; we have shown that standard quaternary DH lasers possess a non-uniform active layer. That is, the more or less standard step-cooled LPE procedure for growing InGaPAs does not result in a quaternary layer of uniform composition. The LPE growth of multi-component III-V semiconductor alloys has been assumed in the earlier work of others to be mainly controlled by diffusion of the solute toward the melt-substrate interface, at least for growth times long with respect to surface attachment kinetic processes. In the present work, $In_{1-x}Ga_xP_{1-z}As_z$ layers have been grown lattice-matched to InP by the step-cooling technique (ΔT=10°C) utilizing, as mentioned above, a growth apparatus that employs a cylindrical slider boat modified so that the slider rotation cycle is executed by a stepper motor under computer control. This system allows an accurate selection of growth times as short as ~9ms and has been used (Ref.9) to grow (~26 ms) quantum-well InGaPAs-InP heterostructure lasers with uniform multiple quaternary layers (11-39 layers) as thin as ~150 Å. In further work (Refs.11 and 12) data have been obtained on quaternary-epilayer-thickness vs growth-time for ultra-short times (e.g., as short as ~9ms) to times as long as ~20s.

For relatively long growth times ($t>1s$) the quaternary layer thickness, as expected, is consistent with diffusion-limited theory. However, for $t<200ms$ the growth rate deviates significantly from diffusion-limited theory, but remains well-behaved and has been, of course, advantageous for the growth of quantum-well layers. For these times, the layer thickness (which is extremely small) is greater than the diffusion-controlled value, and is

characterized by a much weaker time dependence. A state near thermodynamic equilibrium can no longer be assumed to exist at the melt-substrate interface, and interface attachment kinetic processes largely determine the growth rate. As might be expected, the composition of an InGaPAs layer grown for t<200ms (for example, ~18ms) is different (lower gap) than that of a quaternary layer grown for t>200ms (for example, ~1s) at the same temperature from a melt with the same liquidus composition. The experimental data of Refs.11 and 12 (photoluminescence, Auger depth profiles) clearly indicate the existence of two distinct growth mechanisms during more or less standard LPE crystal growth of thick layers (≥1000 Å) by the step-cooling method. This behavior is expected to be general and to characterize all similar LPE growth processes of III-V alloys.

The problem of non-uniform growth of a thick quaternary layer, once identified (this work), can be eliminated (Refs.11 and 12) by constructing a "thick" layer (≥1000 Å) by stacking an arbitrary number of "thin" layers (<200 Å). This has been accomplished and has given preliminary data indicating superior laser performance (Ref.12). This new area of work is in its initial phase and should be continued.

III. LPE QUATERNARY MATERIAL FOR DETECTORS

There has been substantial progress in the development of high quality LPE material for near infrared detectors. The investigation of this quaternary material system has included studies on the effects of lattice mismatch on interface and surface quality, the influence of growth solution dopants on distribution coefficients, the effects of various growth techniques on compositional uniformity, and the effects of growth solution baking time on epilayer purity.

For the growth of quaternary alloy compositions on InP substrates it is clear that the amount of lattice mismatch between the epitaxial layer and substrate should be minimized to obtain good crystallographic quality. We have shown in Ref.13 that the surface morphology is highly dependent on the amount of lattice mismatch for quaternary compositions with a band gap corresponding to a wavelength (λ_g) near 1.3 μm. For this quaternary composition the lattice mismatch must be $\Delta a/a<0.03\%$ to obtain good surface quality, but for epitaxial layers at λ_g=1.15 μm, for example, even with lattice mismatch as large as $\Delta a/a=0.2\%$ the surface quality is reasonably good and there is no melt removal problem at all. However, even though fairly good surface morphology with some lattice mismatch can be obtained for material with λ_g=1.15 μm the interface widths may be significantly broadened, especially for interfaces where InP has been grown on a previously deposited quaternary layer. Reference 14 describes how increased broadening of InP-InGaAsP interfaces (last grown layer listed first) can be correlated with increased lattice mismatch using Auger depth profiling. Only small differences in the chemical transition width of InP-InGaAsP and InGaAsP-InP interfaces have been observed when the lattice mismatch is less than ±0.03%.

Auger depth profiling has also been used to show that significant broadening of InGaAsP-InGaAs interfaces is a result of dissolution of the InGaAs layer by the InGaAsP growth solution. As discussed in Ref.15, growth of a wide band gap quaternary material on InGaAs is difficult because of this dissolution and that this dissolution becomes so severe for increasingly wider band gap quaternary growth solutions that it is impossible to grow InP on InGaAs by LPE. It has been concluded that the dissolution is due to the relatively high diffusivity of arsenic in indium-rich solutions. Thus, growth from a

solution with very little arsenic on a previously deposited layer with a high arsenic concentration results in dissolution of the first layer as arsenic tends to diffuse into the solution.

In experiments on the growth of InGaAsP it has been found that doping the growth solution with any of the three commonly used dopants Zn, Sn, or Te, causes changes in the distribution coefficients of the alloy components. The variation of net carrier concentration and lattice mismatch of Sn, Zn, and Te doped InGaAsP epitaxial layers as a function of X^{ℓ}_{Zn}, X^{ℓ}_{Sn}, and X^{ℓ}_{Te} are reported in Refs. 16 and 17. Since lattice matching is very important in device applications, it is essential that any factors that cause changes in the distribution coefficients be taken into consideration in determining the solution compositions for the growth of lattice matched InGaAsP-InP heterojunctions or quaternary homojunctions.

Considerable work on the effects of various LPE growth techniques on the alloy composition of InGaAsP has been reported in Refs. 18 and 19. Thick constant composition layers can only be obtained using the step-cooling growth technique, and, in general, compositionally graded layers result if any technique involving a cooling rate such as supercooling, equilibrium cooling, or two-phase-solution growth techniques is used. Since the distribution coefficients change with temperature, any growth technique with a constantly changing temperature will result in a compositionally graded layer. In addition, the lattice constant and band gap of epitaxial layers grown using the step-cooling technique are independent of the amount of step cooling but are dependent on the growth temperature. It is shown in Ref. 20 that the thicknesses of InGaAsP and InGaAs epitaxial layers are not severely restricted by the requirement of a fixed growth temperature

and that constant composition layers as thick as 10 μm can easily be obtained. References 19 and 20 give a more complete discussion of the results.

The purity of InP, InGaAsP, and InGaAs epitaxial layers can be significantly improved by proper baking schemes. Using Johnson Matthey grade AlA indium and high purity GaAs, InAs, and InP source materials the net carrier concentration of these layers can easily be reduced to values in the low $10^{15}cm^{-3}$ range. The growth solutions containing properly weighed amounts of GaAs, InAs, and InP added to the pure indium must be baked in the graphite boat for 24 to 48 hrs to obtain these low carrier concentrations. Further baking beyond 48 hrs does not significantly improve either the carrier concentration or electron mobility. In addition, the solution must be baked 3-4 hrs after loading the InP substrate to completely remove any oxygen introduced during loading. The net carrier concentration of InP and InGaAs layers have been reduced to values as low as $3x10^{15}$ and $4x10^{14}cm^{-3}$ respectively with liquid nitrogen mobilities of 40,000 and 48,000 cm^2/V-sec respectively.

A Be-implanted 1.3 μm InGaAsP avalanche photodiode has been fabricated with an avalanche gain $\geq$100 and breakdown voltage of ~120 volts. This photodiode had a leakage current less than 1 μA up to 100 volts which was less than what had been previously reported for this quaternary composition, although this is still rather high for good avalanche photodiodes. Reference 21 provides the details of the fabrication procedures and results. In more recent work we have been able to greatly reduce leakage currents by using an InP p-n junction for multiplication and an InGaAsP or InGaAs layer for absorption. The thermal generation rate and the probability of band to band tunneling are reduced by the wide band gap InP material which results

in a much smaller leakage current. If the ratio of the hole ionization coefficient and the electron ionization coefficient in InP is larger, this will also allow higher avalanche gain and lower excess noise factors. Current research is concentrated on developing these new structures for low leakage, high gain, avalanche photodiodes.

IV. VAPOR PHASE GROWTH OF (In-Ga-As-P) ALLOYS AND COMPOUNDS

Until recently the infrared emitter and detector structures in the InGaAsP alloy system of interest in optical fiber communication systems were grown exclusively by the liquid phase epitaxial growth techniques. Vapor phase epitaxy has several advantages over liquid phase epitaxial growth.[22-24] Excellent control of the uniformity and reproducibility of layer thickness, composition, and doping level is generally achieved. There are no problems with melt wipe-off or meniscus line defects. The surface morphology is easier to control and the vapor phase technique is also more suitable for large scale epitaxial growth. There are three major vapor phase growth techniques that can be used to grow these compounds: (1) the organometallic system[25-34] (TMG-TEI-AsH_3-PH_3-H_2), (2) the halide system[35-44] (PCl_3-$AsCl_3$-H_2-In-Ga), and (3) the hydride system[45-58] (AsH_3-PH_3-HCl-H_2-In-Ga). The hydride system which had shown great flexibility in the growth of ternary III-V compounds[59] was used in this study.

A. SYSTEM DESCRIPTION AND DESIGN CONSIDERATIONS

The vertical furnace tube is shown schematically in Figure 1 and consists of: (1) two quartz tubes which hold the gallium and indium source boats (source zone), (2) a large quartz tube which includes a mixing zone, deposition zone, and a preheat zone, (3) a heated exhaust line, and (4) a detachable magnetic sample lifter and rotator (pedestal assembly). The five temperature zones illustrated in Figure 2 use separate conventional, resistance heated furnace elements. The system is vertical primarily due

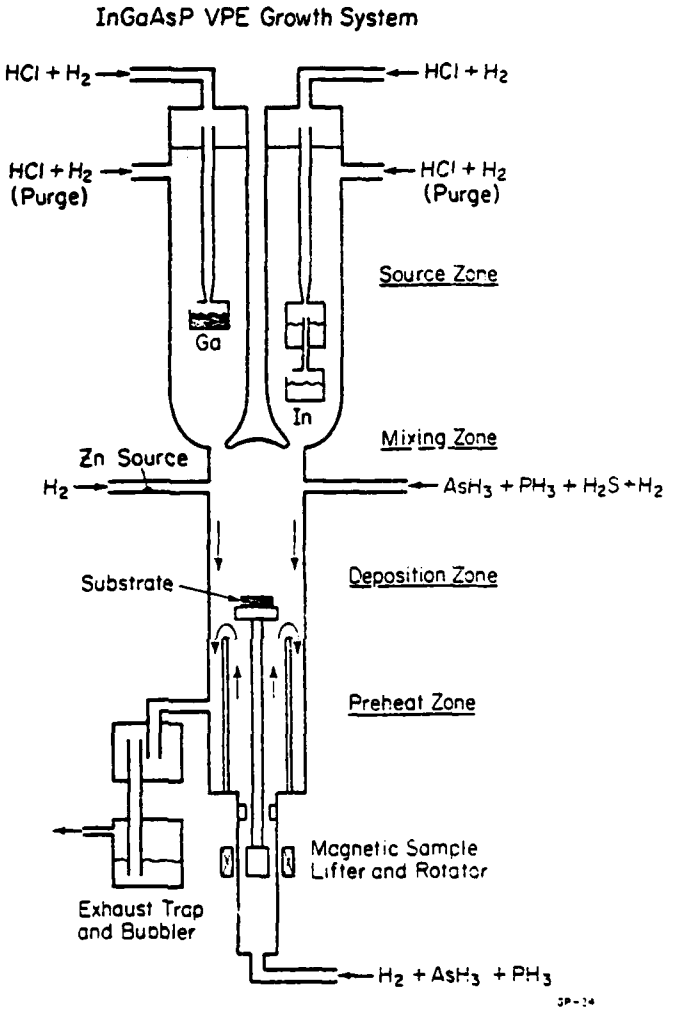

Figure 1. Original vapor phase reactor schematic.

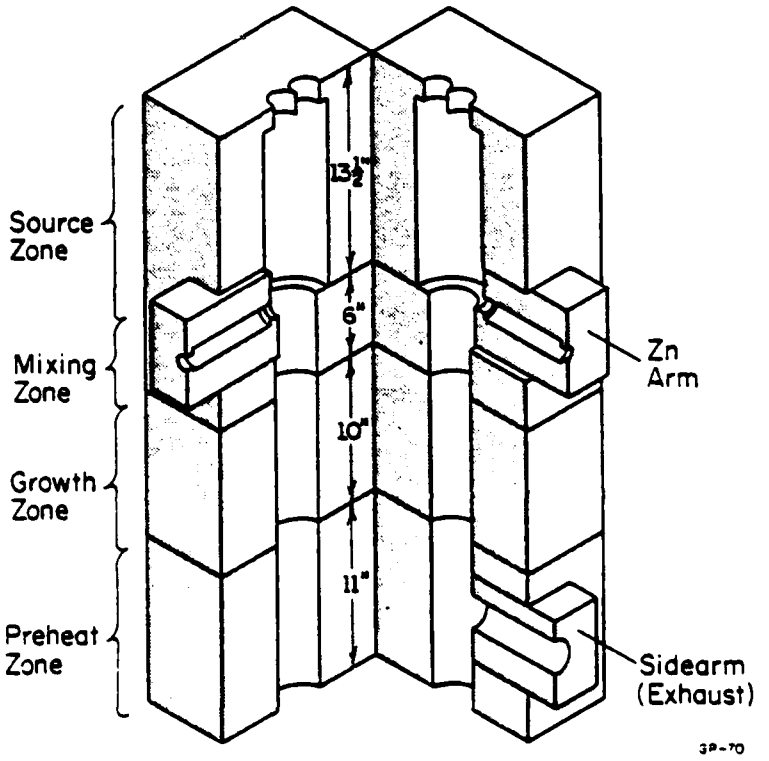

Figure 2. Vertical furnace schematic.

to space limitations, although this arrangement also makes it easier to mechanize the substrate holder for rotation and lifting.

The design of the source boats is one of the most critical considerations in the design of the system. Ideally, all of the HCl that is introduced over the gallium and indium boats should be converted to GaCl and InCl because the alloy composition of $In_xGa_{1-x}As$ and $In_xGa_{1-x}As_yP_{1-y}$ is directly affected by the InCl/GaCl gas flow ratio.[60-61] It is imperative that this ratio, which is typically >1 for alloy compositions of interest, be constant otherwise compositional inhomogeneities will occur. The ratio must be >1 because of the greater relative stability of InCl to GaCl in the temperature range of interest, and hence more InCl is required for typical growth conditions.[61] In a horizontal system like RCA's a large volume of each metal and a long reaction path length are used to ensure nearly complete conversion of HCl to GaCl and/or InCl.[62] The reaction efficiency also depends upon the flow rate of the gas (H_2 + HCl) over the boat (i.e. the residence time of the HCl over the sources)[63] and temperature. Contact between the HCl and the source metals can also be increased by using deflection baffles and this should increase the reaction efficiency. Typical surface areas of the metal sources used by RCA range from 25-35 cm^2.

In the vertical system it is not feasible to use a single stage structure of this area as it would require a boat with a diameter of 62 mm and would require a main furnace tube about twice the diameter that we are currently using. Instead, to obtain a reasonable surface area two stages were stacked together to form the boat shown in Figure 3. The surface area contained in 1 stage is approximately 7 cm^2. Thus the indium or gallium surface area in the vertical system is about 1/2 the surface area in the horizontal system. An advantage that the vertical boat design has is

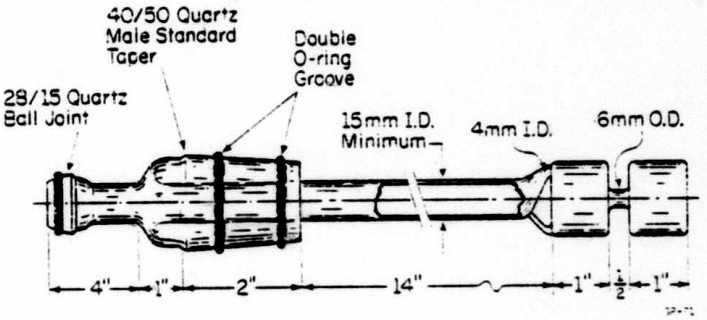

Figure 3. Source boat design.

that each stage is closed (i.e. the gas is confined). Thus, there should be better contact between the HCl gas and the metal surface. At the same time, however, the flow rate in the source boats, must not be so high that the residence time is insufficient for complete reaction or that it forces the gallium and/or indium out of the boat and into the main tube.

Unlike most other vapor phase reactors this vertical system is kept hot at all times (except when loading the gallium or indium). For loading the substrate prior to growth or removing it after growth, a high purity N_2 blanket is maintained around the base of the furnace during the time the magnetic sample lifter is detached from the furnace tube, and H_2 flows are maintained through both the pedestal assembly and the upper part of the reactor. A peristaltic pump, which is connected to the exhaust line, removes a portion of the H_2 flow from the upper part of the system while the rest of the H_2 flows out of the base of the furnace tube. The H_2 flows from the upper and lower parts of the reactor along with the N_2 blanket minimize the oxygen contamination of the system during substrate loading. This arrangement permits a fast turnaround time between growth runs.[64-65]

After the substrate is loaded, the system is purged for 30 minutes with H_2. Then the sample is raised into the preheat zone in which a H_2-AsH_3(PH_3) ambient has been established to prevent thermal damage to the substrate (or to grown layers).

While the sample is in the preheat zone, separate streams of HCl are introduced over the gallium and indium source boats. The HCl reacts with the gallium and/or indium metal sources to form GaCl and/or InCl which are (is) transported downstream by H_2.[63] In the mixing zone the metal chlorides are mixed with AsH_3 and/or PH_3 (10% in H_2). When the gas compositions are established the sample is raised into the growth zone to initiate growth. A typical temperature profile used for InP growth is shown in

Figure 4.

A schematic diagram of the initial semi-automatic gas control system is shown in Figure 5. The H_2S dopant system, HCl, AsH_3, and PH_3 flow rates were regulated by Tylan mass flow controllers and borosilicate glass flowmeters were used to set all the other gas flows. The 316 stainless steel gas lines were connected with compression fittings.

B. FACTORS AFFECTING PURITY

Comprehensive studies of the factors that affect the purity of VPE grown material have been done. Five major parameters control the purity of III-V compounds: (1) purity of starting materials,[66-68] (2) atmospheric contamination,[67,69] (3) mole fraction effect,[70-76] (4) substrate and source temperature,[37,78] and (5) substrate orientation.[52,77]

The purity of the starting materials used is the highest commercially available. Hydrogen is purified by passing it through a palladium-alloy diffuser. The HCl gas is 99.999% pure, the 10% AsH_3 in H_2 is 99.9995% pure and the 10% PH_3 in H_2 is 99.9995% pure. The gallium (Alusuisse Metals Inc.) and indium (Johnson-Matthey Metals Ltd.) both have a reported purity of 99.9999+%. All of the quartz tubing used in the reactor is commercial grade quartz (Heraeus-Amersil, Inc.) which has an average metallic impurity content of 30 ppm. Synthetic quartz like Suprasil or Spectrosil which has an average metallic impurity content of less than 1 ppm can provide a higher purity reactor once the final design is established.

The entire gas flow system was helium leak tested and found to have a leak rate of less than 10^{-6} atm-cc/sec. This rate is similar to those reported for other high purity systems.[79,80]

The most important parameter for controlling the purity of III-V VPE layers is the mole fraction (the number of moles of one component divided by the total number of moles of all components) effect. This effect is

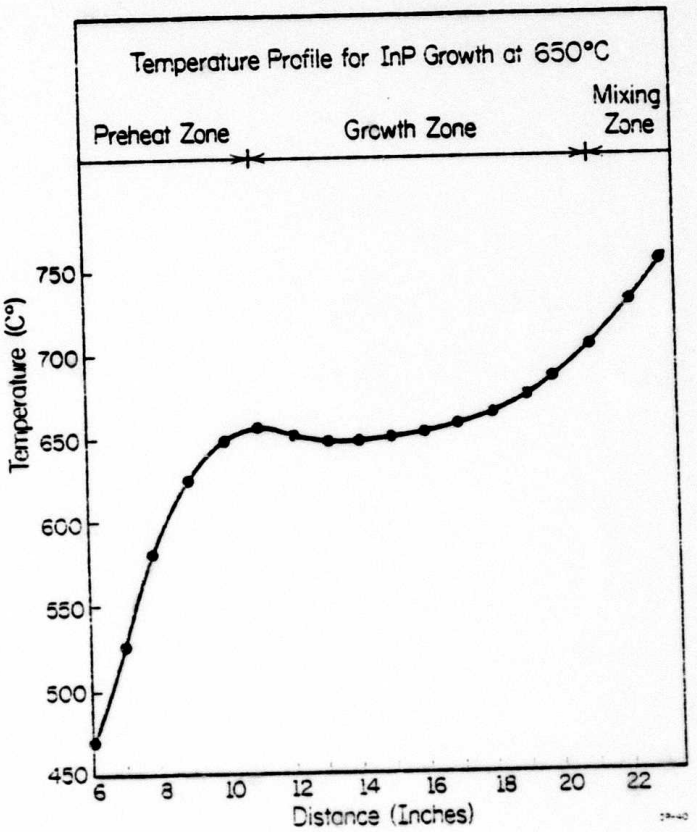

Figure 4. Vertical temperature profile. Growth occurs at a distance of 15" from the bottom of the furnace.

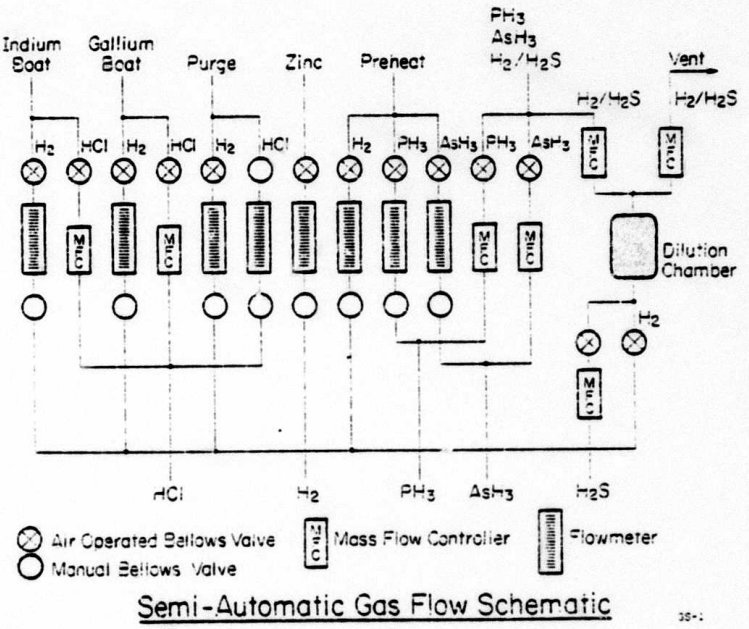

Figure 5. Original gas flow schematic.

seen as an inverse dependence of the free carrier concentration on the partial pressure of one or more of the transporting components (e.g., P_{AsCl_3}, P_{AsH_3}, P_{HCl}), and occurs because chlorosilanes are generated by the reaction of HCl and H_2 with hot quartz. This process is believed to determine the amount of silicon that is incorporated in III-V epitaxial layers.[73,81]

In the hydride system, unlike the halide system, both the metal chlorides and hydride mole fractions can be separately controlled. These mole fractions can be increased either by increasing the individual gas flow rate or by decreasing the total H_2 carrier gas flow rate (which is by far the largest flow rate in the system). However, because of reactor gas flow dynamics it is not clear that both of these methods will produce the same carrier concentrations and mobilities. In addition, unlike the halide system where the III-V ratio is essentially fixed at 1.9,[73] the III-V ratio in the hydride system[82] can be varied over a wide range. It is known that the III-V ratio can influence certain fundamental parameters such as minority carrier lifetimes, diffusion lengths, and certain trap concentrations.

For the growth of GaAs it has generally been found that the lowest substrate temperature produces the purest material for a given set of flow rates provided that a good crystal structure was maintained.[37] The effects of the substrate temperature on purity is unknown for InP, $In_xGa_{1-x}As$, and $In_xGa_{1-x}As_yP_{1-y}$. Typical growth temperatures for GaAs are in the 700-775°C range and for InP and $In_xGa_{1-x}As$ (on InP) typical growth temperatures are in the 650-750°C range.

The source temperature is important because it can affect the purity of the source and also because it is one of the controlling factors of the reactivity of the source with HCl. Path length and gas velocity are also important. Too high a source temperature will cause contamination of the

source material with silicon from the quartz while too low a source temperature will result in a large amount of unreacted HCl and not enough GaCl (InCl) for growth. Typical gallium and indium source temperatures are in the 750-800°C range.

Substrate orientation also affects the sample purity.[37] The highest purity GaAs samples have been grown on (211)A substrates or on substrates which were misoriented from the <100> by 5° or 6° towards the <110>. The substrate orientation also affects the growth rate, compensation, and surface morphology, with higher growth rates, lower compensation, and better surfaces obtained with an orientation 2° to 5° off <100> toward the <110> or higher index planes.

C. GaAs GROWTH

The vapor phase growth system was initially used to grow GaAs epitaxial layers. These undoped layers were grown on Cr-doped GaAs substrates misoriented 2° off (100) → (110). The growth temperature was 725°C. Epitaxial growth occurred the very first time the system was used. The average growth rate for n-type non-intentionally doped samples was 0.20 μm/min and for p-type non-intentionally doped samples the growth rate was 0.08 μm/min. The substrate preparation consisted of removing 4 mils from the GaAs substrate using a 1% bromine-methanol solution and then etching the substrate in hot HCl for 5 minutes before rinsing in water and isopropyl alcohol and blowing dry with high purity N_2. The samples were then loaded into the system using the procedure described above. Besides the conversion problem, stacking faults as depicted in Figure 6 were sometimes observed on the surface and in cross sections of the grown layers. These defects have been attributed to impurities on the surface.[83-86] An etching step using either a $5H_2SO_4:H_2O_2:H_2O$ solution or *in situ* HCl etch probably would have taken care of these problems. It was also observed that the

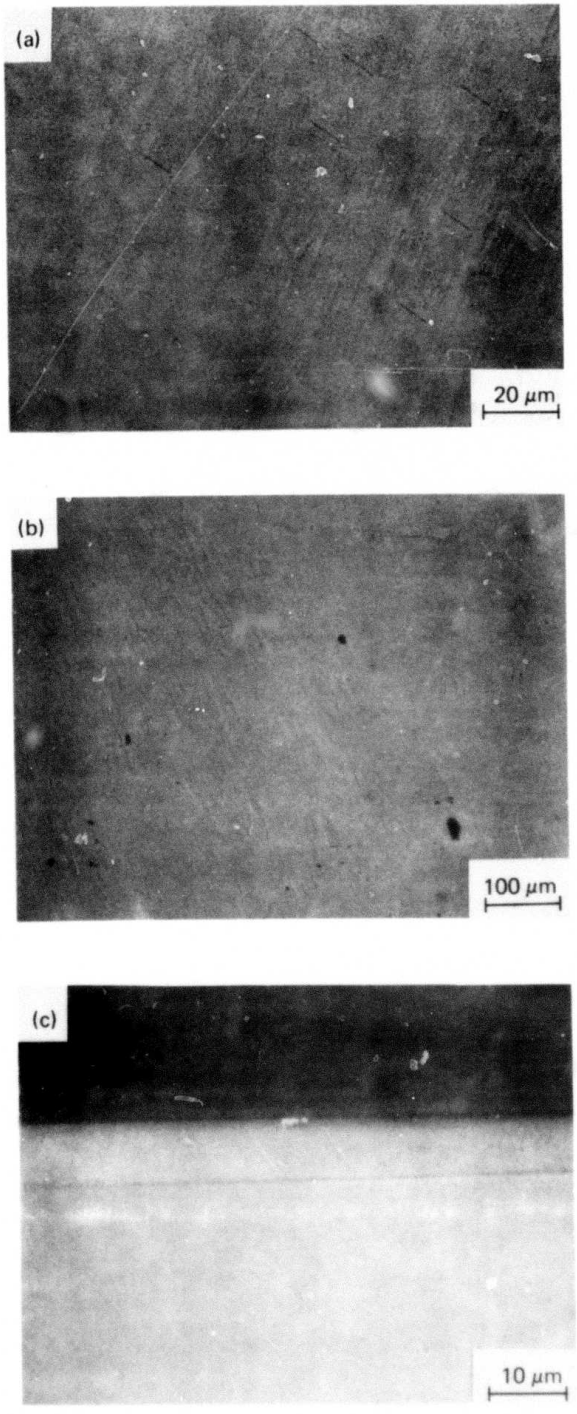

Figure 6. (a) and (b) Examples of stacking faults on the surface; (c) cross section through a stacking fault.

compensation ratio decreases for an increasing III-V ratio as shown in Table 1. Figure 7 illustrates the mole fraction effect in the hydride system for the growth of GaAs. Several samples were grown with carrier concentrations in the range of $7\text{-}11 \times 10^{14}$ cm^{-3} (77°K) and liquid nitrogen mobilities 75,000 cm^2/Vs. The highest room temperature mobility was 6800 $cm^2\ V^{-1}s^{-1}$ with an average room temperature mobility of 4500 $cm^2\ V^{-1}s^{-1}$.

The low growth rates obtained in this initial work were due to the high carrier gas flow rate used over the gallium boat. That this was in fact true became apparent when, in the first InP growth attempt, the same (H_2 + HCl) gas flow rate used for GaAs resulted in incomplete reaction between the indium and HCl and the InP substrate was severely etched.

D. InP GROWTH

The characterization of the vapor phase system was continued by growing undoped InP layers on Cr-doped (Metals Research), and Fe-doped, nominally (100) oriented InP substrates (N.R.L.) and on Fe-doped substrates intentionally misoriented 3° off (100) toward (110) (Metals Research). The growth temperature was 650°C.

Indium phosphide substrates were prepared for growth by first etching 1 1/2 - 2 mils of InP from one side of the substrate, using a 4% Br/methanol solution. This side was used as the back surface to prevent the work damage on this side from propagating into the grown layer. The other side was chemically-mechanically polished with a 1% Br/methanol solution, to remove 4-5 mils of material. In initial work the polished substrate was etched for 2 minutes in 1% Br/methanol just before growth. This proved to be unreliable because the etch would occasionally produce small hillocks on the surface and if the substrate were exposed to air for sometime, a white haze (probably caused by an oxide) would appear on various parts of the substrate. It was later found that a one hour soak in a solu-

TABLE 1

III/V Ratio versus Compensation Ratio

Sample	n(77°K) (cm^{-3})	μ(77°K) ($cm^2V^{-1}s^{-1}$)	Ga/As	N_A/N_D (77°K)
28	1.92×10^{15}	16,170	0.515	0.76
30	2.28×10^{15}	33,744	0.541	0.44
33	8.28×10^{14}	73,561	0.860	0.26

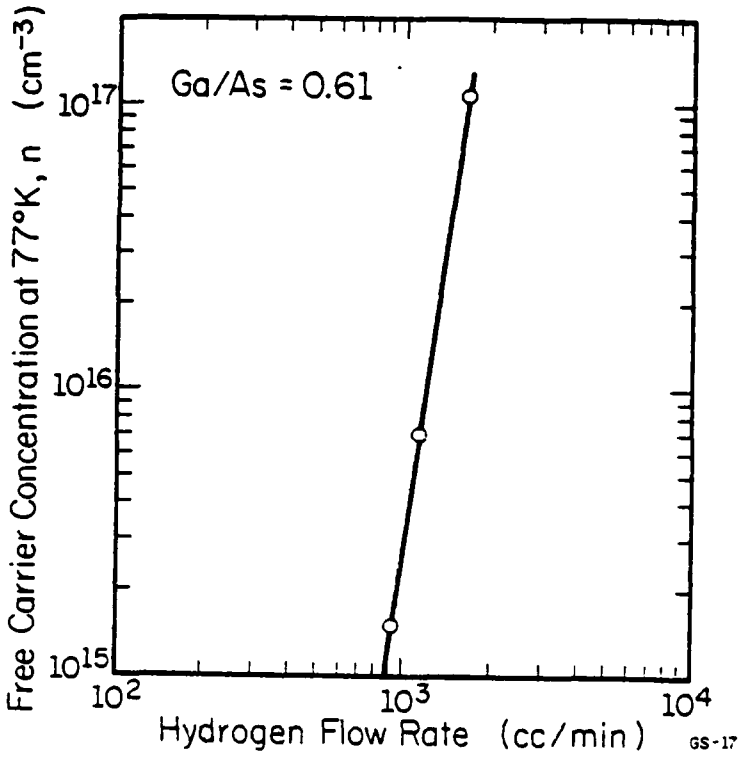

Figure 7. Free carrier concentration, n (cm^{-3}), at 77°K versus the hydrogen flow rate (cc/min).

tion of KOH(45w/o sol.)[87] was effective in removing oxides from the InP surface. A cooled 1% Br/isopropyl solution was also tried and produced a much better polished surface than the 1% Br/methanol solution.

The average InP growth rate in this initial work was 0.04 μm/min which is very small for the hydride system. These samples had mirror-like surfaces but were heavily compensated.

By reducing the H_2 flow over the indium melt (which decreased the gas velocity over the indium and gave more time for the HCl to react with the indium and form InCl), and by decreasing the mixing zone temperature, the growth rate increased to 0.5 μm/min. The lower mixing zone temperature presumably caused less decomposition of PH_3 into P_2 and P_4 and since InCl tends to react more with PH_3 than with P_2 and/or P_4 resulted in the higher growth rate. Ban and Ettenberg (RCA) noted the same characteristic in their work on $In_xGa_{1-x}P$.[88]

The epitaxial layers grown with this higher growth rate still displayed very flat surfaces. The surface morphology of layers grown on Fe-doped substrates tended to be slightly better than those grown on the Cr-doped substrates. The surface morphology also tended to be slightly better on the misoriented Fe-doped substrates than on the oriented ones. It is possible that a still larger misorientation (5-6° off <100> toward <110>) as often used for GaAs $AsCl_3$ VPE growth would produce even better surface morphology.

Besides the substrate orientation, the surface morphology of InP layers depends upon the relative amounts of InCl and PH_3 that are in the gas streams. Too high of an InCl concentration will cause hillocks on the surfaces of grown layers while too low a concentration of InCl will cause pitting. The amount of PH_3 present seems to determine the size and density of the above defects. Figure 8a shows an InP surface covered with hillocks

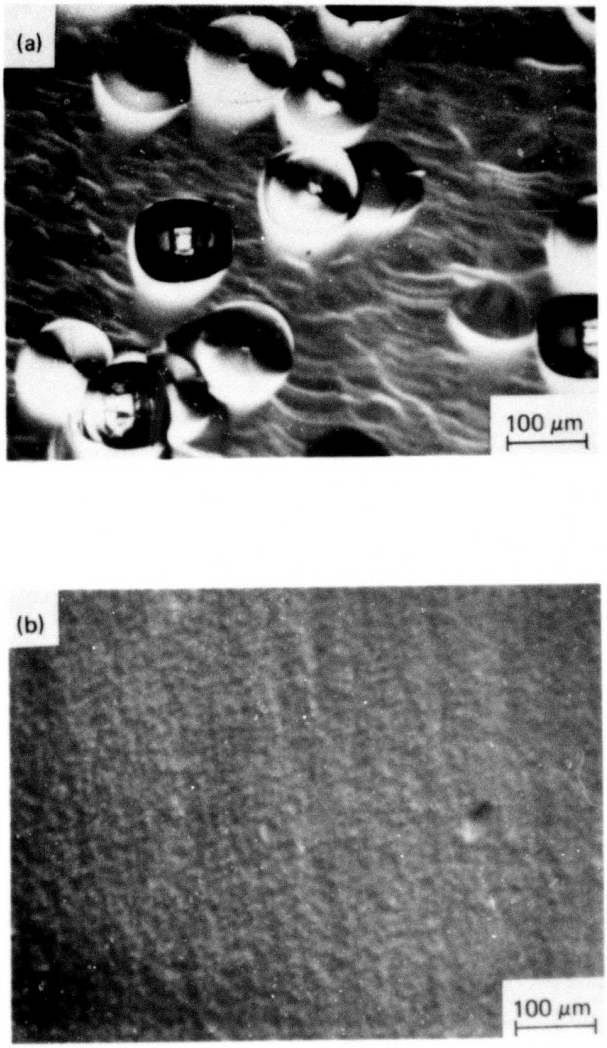

Figure 8. (a) InP surface morphology due to an excess of InCl; (b) InP surface morphology with PH_3 flow rate increased by 20%.

while Figure 8b shows the effect of increasing the PH_3 flow by 20% while keeping the HCl flow constant.

Epitaxial layers have been grown on several substrates simultaneously during a given run, and all of the samples have similar characteristics. Carrier concentrations have been in the $8\text{-}12 \times 10^{15}$ cm^{-3} range with an average room temperature mobility of 3,200 cm^2/Vs and an average liquid nitrogen mobility of 20,000 cm^2/Vs. The highest mobility obtained to date is 30,000 cm^2/Vs (77°K). These samples also displayed less compensation than the first samples grown, possibly due in part to the higher III-V ratio that was used (III-V=1). Figure 9 shows the 77°K mobilities and carrier concentrations superimposed on theoretical curves of mobility vs. carrier concentration for various compensation ratios.[89]

The variation of the growth rate of InP epitaxial layers grown at 650°C with total H_2 flow rates between 500 and 900 sccm (2-3 liters/min is commonly used in most hydride systems of similar dimensions) for III-V gas ratios of 1 and 2 was investigated. Layers grown with a III-V gas ratio of 2 tended to have more hillocks on their surfaces and displayed less compensation than layers grown with a III-V ratio of 1. The growth rate varied from 0.63 μm/min to 1.82 μm/min (Figure 10) for a constant HCl partial pressure of 30×10^{-3} atm and a constant PH_3 partial pressure of 15×10^{-3} atm as the total H_2 flow rate was reduced from 900 sccm to 500 sccm. Other layers were grown with a constant HCl and PH_3 flow rate of 13.5 sccm while the total H_2 flow rate was reduced from 900 sccm to 500 sccm (Figure 11). The growth rate dropped from 1.25 μm/min to 0.7 μm/min tending to support a mass transport limited growth mechanism for InP using the hydride system.

Hall effect measurements on these samples indicated a large carrier freeze-out between 300°K and 77°K (2.2×10^{15} cm^{-3} to 5.7×10^{14} cm^{-3}). A careful check of the gas flow system indicated that leaks had developed

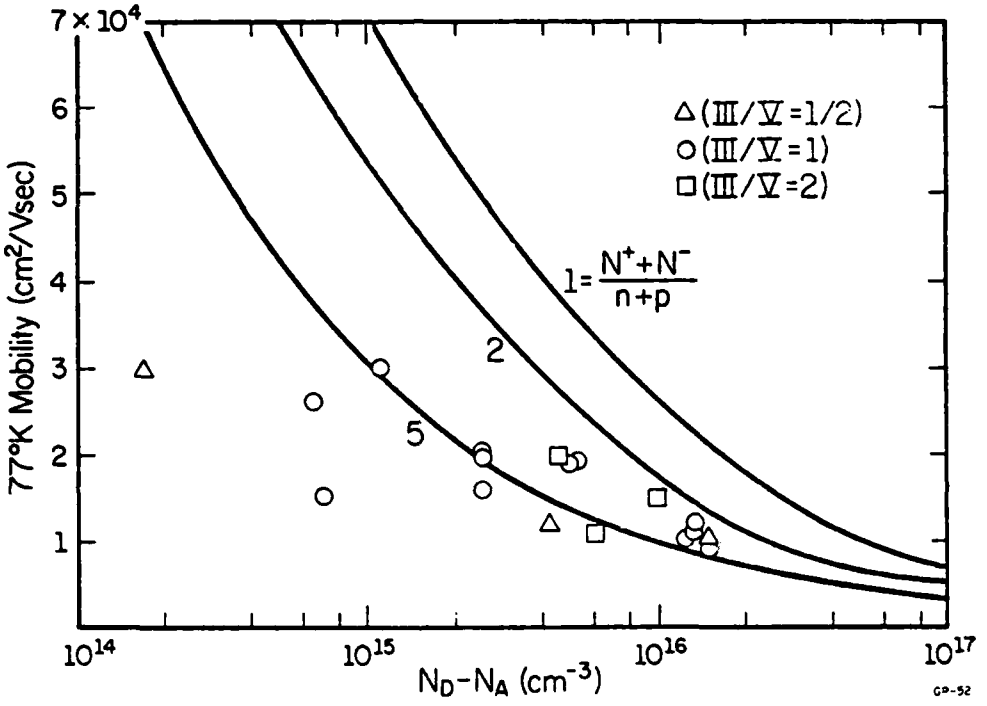

Figure 9. Mobility vs. free-electron concentration in InP for various III/V gas ratios at 77°K for compensation ratios of 1, 2, and 5.

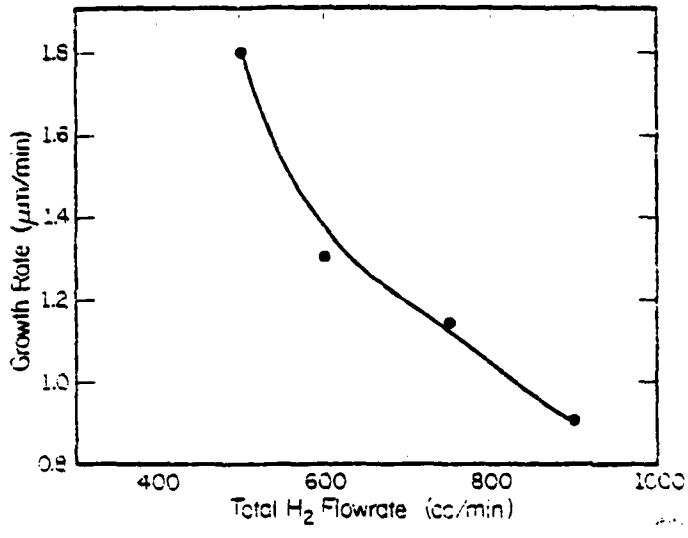

Figure 10. Growth rate for constant HCl and PH_3 partial pressure (P_{HCl} = 30 x 10^{-3} atm, P_{PH_3} = 15 x 10^{-3} atm).

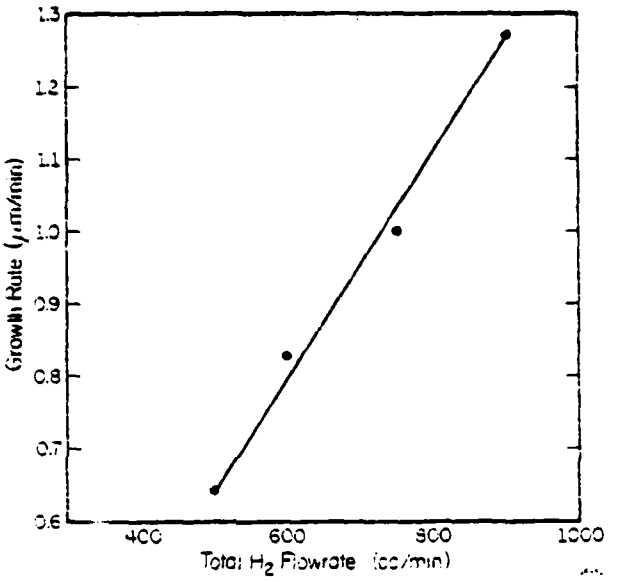

Figure 11. Growth rate for constant HCl and PH_3 flow rates (HCl = PH_3 = 15 sccm).

around the O-Ring seals in the HCl mass flow controllers and that the HCl regulator also was leaking. To eliminate these problems the gas flow control system was modified as described in the next section.

E. AUTOMATIC GROWTH SYSTEM

Several other problems were encountered during the use of this early version of the vapor phase system. Due to the use of the borosilicate glass flowmeters the system could not be totally computer controlled. Also, due primarily to the restricted space for the gas flow section of the VPE system many of the compression fittings were too close together which made it difficult or impossible to maintain the leak integrity of the compression fittings in the gas flow system.

So that the gas control system could be fully automated all the borosilicate glass flowmeters were replaced with mass flow controllers as shown in Figure 12. Table 2 lists the flow ranges of the mass flow controllers used in the system. The solid zinc source for p-type doping was replaced with diethylzinc for more flexible p-type doping. More abrupt doping concentration changes and less residual contamination should be possible with this doping source. The automatic gas flow system has the capability of adding excess HCl, NH_3, and O_2 to the reactor during growth. These substances are known to influence the purity of III-V compounds.[90-94] The influence of these materials on carrier concentration, mobility, compensation ratio, and composition of $In_xGa_{1-x}As$ and $In_xGa_{1-x}As_yP_{1-y}$ will be studied in further work with the system. Excess HCl can be used to prevent growth on the furnace tube which is essential for maintaining constant composition during the growth of $In_xGa_{1-x}As$ and $In_xGa_{1-x}As_yP_{1-y}$. There is also separate control over the flow rate in each purge section. These changes are illustrated in Figure 13 while Figures 14-17 show pictures of the new system.

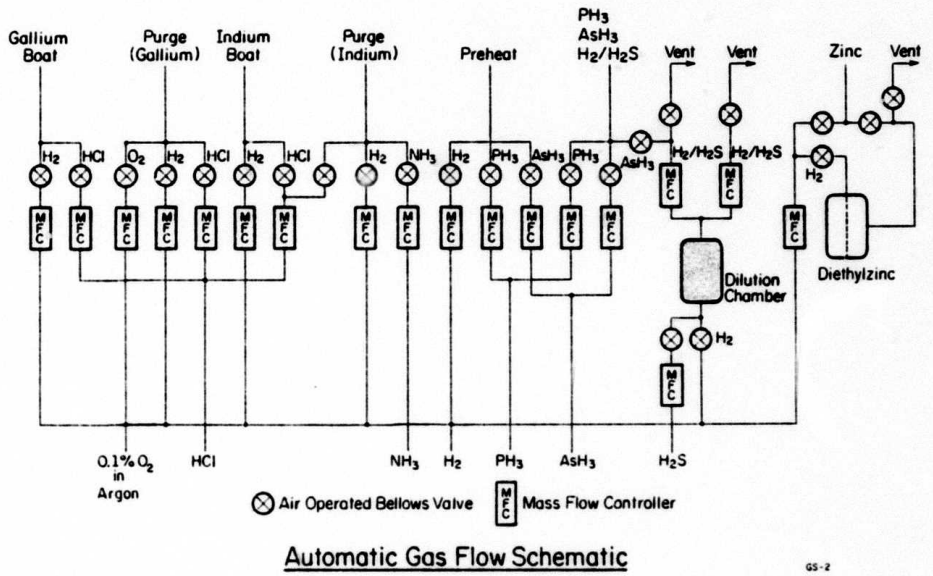

Figure 12. New gas flow schematic.

TABLE 2

Mass Flow Controllers in Automated System

Mass Flow Controller	Flow Range (sccm)
HCl (Indium Boat)	2-100
HCl (Gallium Purge)	0.2-10
HCl (Gallium Boat)	0.4-20
H_2 (Indium Boat)	2-100
H_2 (Gallium Purge)	20-1000
H_2 (Gallium Boat)	2-100
H_2 (Indium Purge)	40-2000
H_2 (Preheat)	20-1000
H_2 (Diethylzinc)	4-200
10% AsH_3 in H_2 (Preheat)	10-500
10% AsH_3 in H_2 (Growth)	10-500
10% PH_3 in H_2(Preheat)	6-300
10% PH_3 in H_2 (Growth)	10-500
H_2/H_2S (Gaseous Dopant)	2-100
H_2/H_2S (Dilute Gaseous Dopant Mix)	2-100
H_2/H_2S (Dilute Gaseous Dopant Vent)	40-2000
NH_3 (Indium Purge)	4-200
1000 ppm O_2 in Argon (Gallium Purge)	4-200

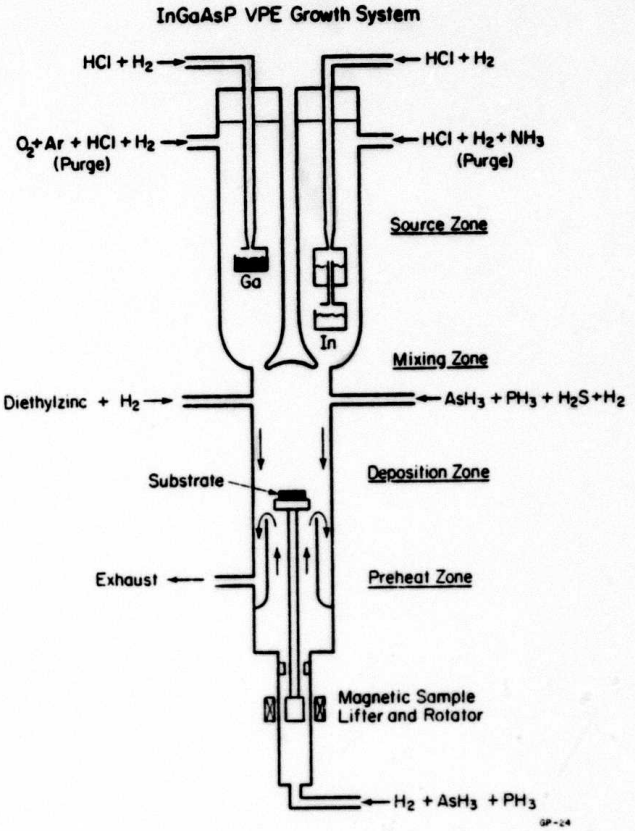

Figure 13. New vapor phase reactor schematic.

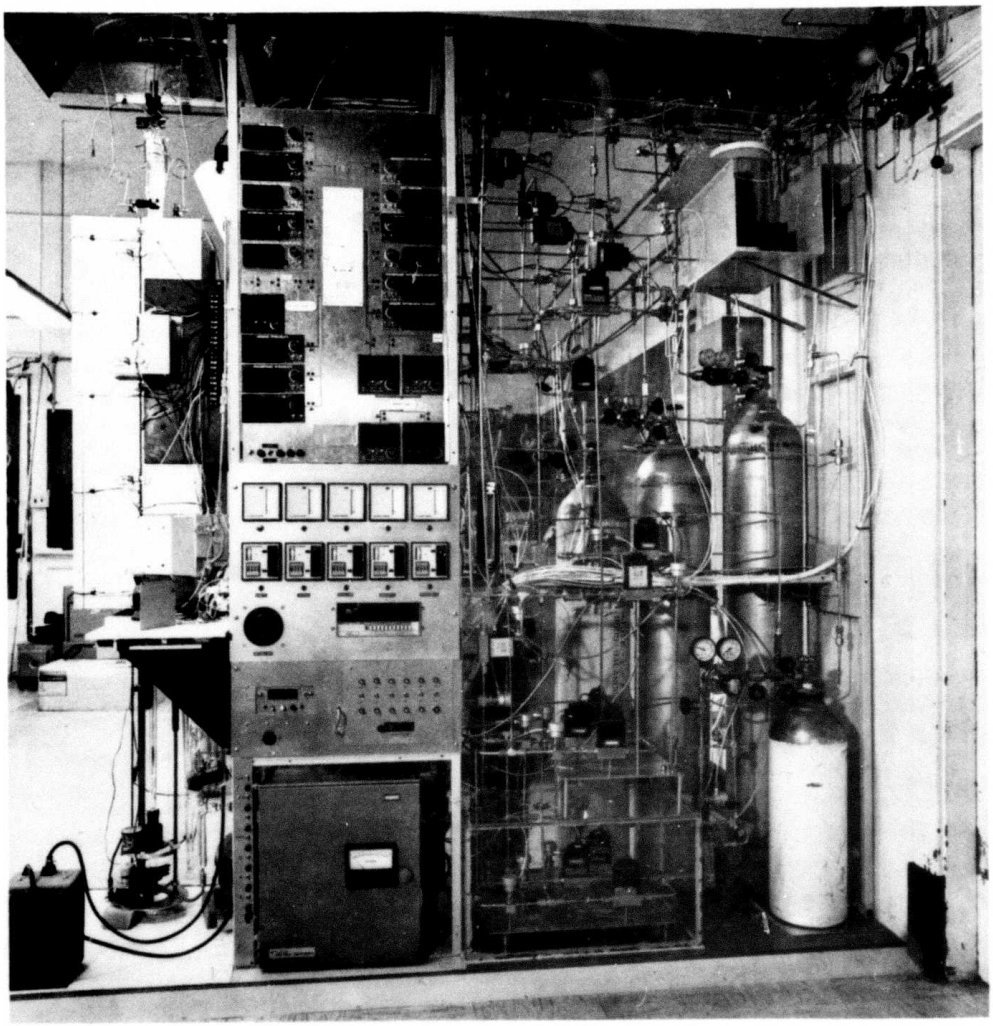

Figure 14. Front view of new automated system.

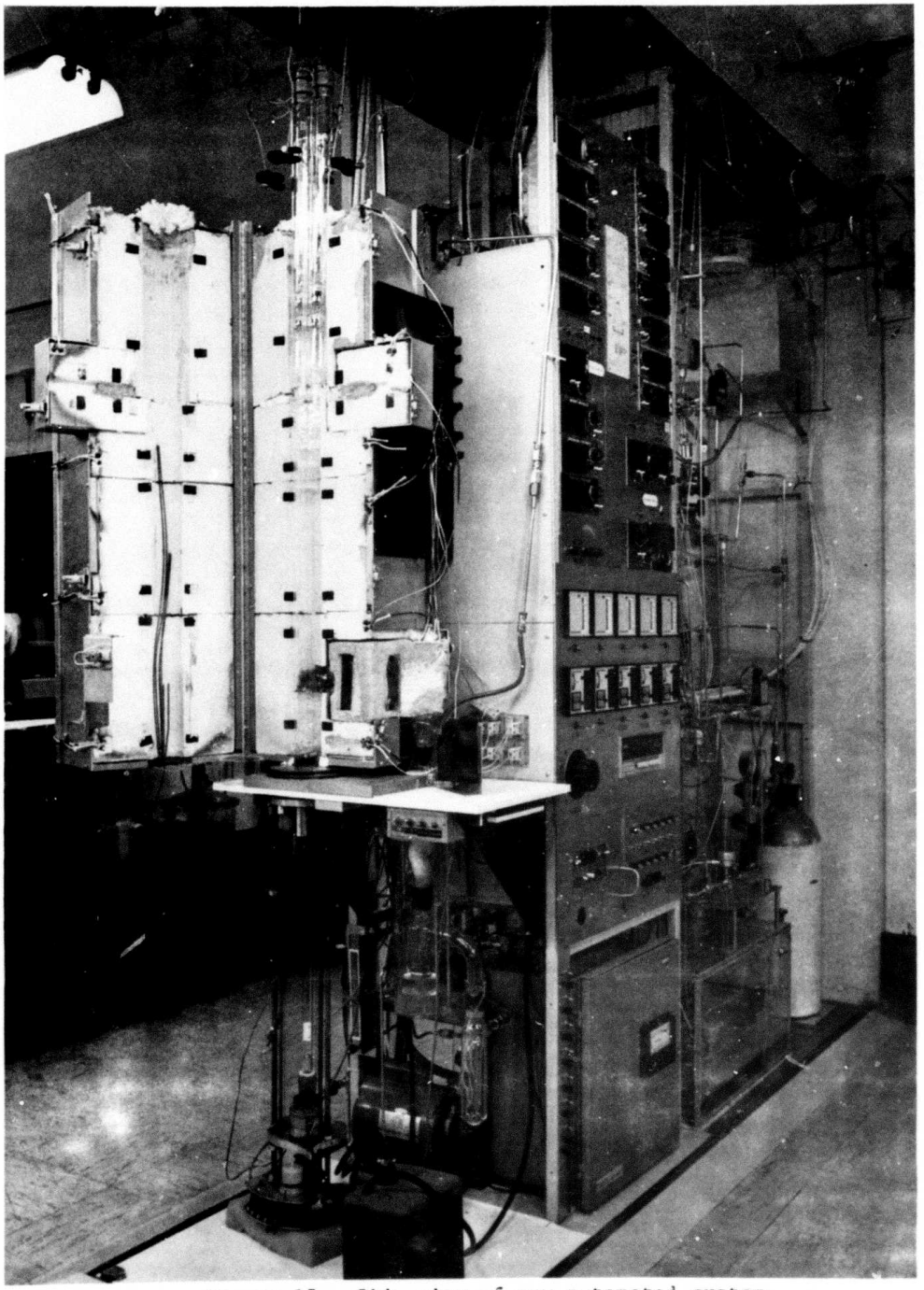

Figure 15. Side view of new automated system.

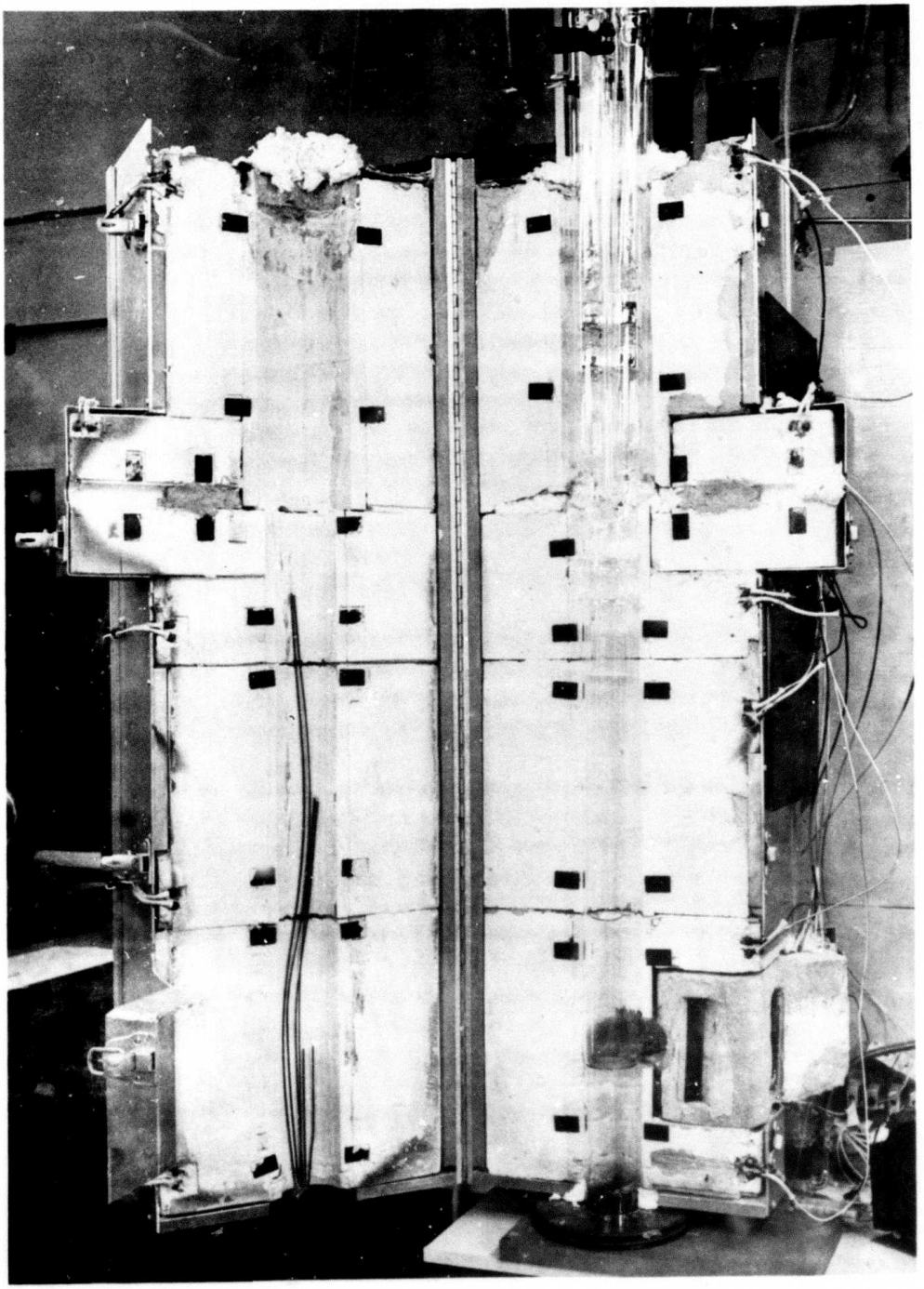

Figure 16. Vapor phase reactor.

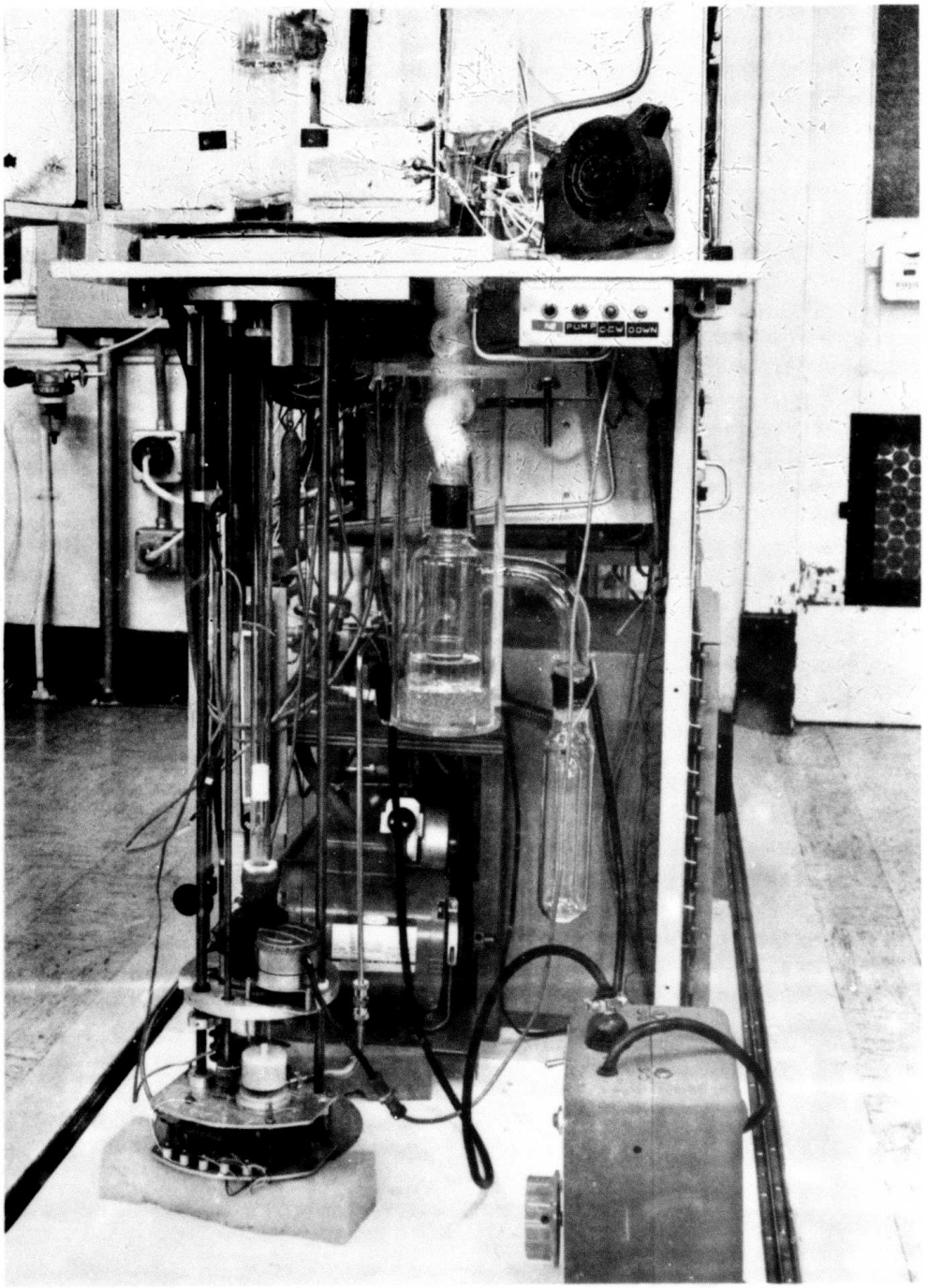

Figure 17. Pedestal assembly and exhaust system.

To increase the leak integrity and reliability of the system, most of the compression fittings in the gas system were eliminated and replaced with welded VCR (Nupro) fittings. Since the tubing was welded, scratches on the tubing (which can cause leaks if compression fittings are used) and the hardness of the stainless steel tubing were not important. Nupro air operated bellows valves were used to turn gas flows on and off. The system was helium leak tested and had a leak rate of less than 10^{-9} atm-cc/sec, an improvement of 3 orders of magnitude over the semi-automatic system.

More precautions were also taken to eliminate any possible contamination problem in the HCl section of the system. The Viton O-Rings in the HCl mass flow controllers were replaced with teflon O-Rings since in the semi-automatic system HCl appeared to have attacked the Halocarbon grease (which is supposed to be inert and is used for lubrication). All of the HCl mass flow controllers are enclosed in a high purity nitrogen box so that if a leak does occur its effects should be minimized.

Figure 18 shows the high purity gas system. Most of the gas regulators are single stage and made of 316 stainless steel. The HCl regulator which is designed to be corrosion resistant has a nickel coated brass body with internal parts constructed of monel. This regulator is protected by a submicron filter placed just before the cross purge assembly which is used to prevent contamination and possible failure of the regulator. These filters have an efficiency of 99.999% for particles 0.3 microns and larger and an efficiency of 99.997% for particles 0.03 microns and larger. Their primary purpose is to trap any particulate coming from the gas cylinder which otherwise would plug the gas sensors of the mass flow controllers. The other regulators are also equipped with a cross purge assembly which eliminates the escape of toxic, corrosive and/or flammable gases when the

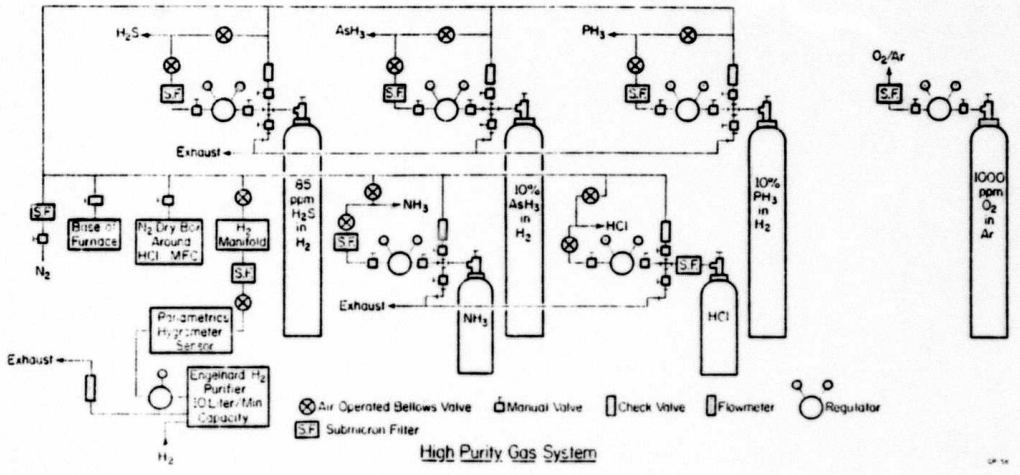

Figure 18. High purity gas system schematic.

regulator is disconnected from the cylinder, and at the same time prevents atmospheric contamination of the regulator and gas lines.

In the present high purity gas system all gas lines can be purged with high purity nitrogen either through the cross purge assemblies on the regulators or just beyond the output of the regulator using an interconnecting N_2 purge line.

The water vapor at the output of the H_2 purifier is monitored by a Panametrics hygrometer sensor. Water vapor concentrations as low as 1 part per billion can be detected with this sensor. All other gases used in the system are the highest purity gases that are commercially available. Typical impurities found in these gases are listed in Table 3.

During the study of the gas flow rates and III-V ratios in the VPE growth system problems were encountered with blockage of the reactor exhaust line. To minimize these problems the system was initially modified in two ways: (1) a hydrogen line was added to the furnace tube in the vicinity of the blockage in an attempt to increase the gas velocity and turbulence in this region so as to prevent the blockage; and (2) a cold trap was added to the output of the bubbler to prevent blockage in the stainless steel exhaust line. Although the cold trap prevented blockage in the vent line, the additional hydrogen line did not prevent the blockage at the output of the reactor. The exhaust section was again modified as depicted in Figure 19 by adding a dump tube in the sidearm. The purpose of the dump tube in the sidearm is to have the deposits form inside it so as to be able to readily remove this section without disturbing the main tube. Since the furnace heating element ends before the 90° bend in the sidearm, the furnace tube was wrapped with high temperature (870°C) heating tape in this region. This insured that the blockage occurred inside the dump tube. The Halocarbon grease which is used to seal the exhaust sidearm to the top

TABLE 3

Typical Impurities Found in High Purity Gases

Gas	NH_3	HCl	AsH_3, PH_3	O_2	Ar
Supplier	Linde	Synthatron	Phoenix Research	Synthatron	Synthatron
Purity	99.999%	99.999%	99.9995%	99.998%	99.9995%
Typical Impurities	N_2<8 ppm	N_2<4 ppm	Ar, N_2<1 ppm	N_2,Kr<15 ppm	H_2O<3 ppm
	O_2<2 ppm	O_2<1 ppm	H_2O,O_2<1 ppm	Ar<10 ppm	N_2<2 ppm
	H_2O<5 ppm	H_2O<1 ppm	CO,CO_2,C_2H_2<1 ppm	H_2O,CH_4<3 ppm	O_2,CH_4<1 ppm
	CH_4<1 ppm	CO_2<1 ppm	C_2H_6,C_3H_8<1 ppm	H_2,CO_2<1 ppm	THC,CO_2<1 ppm
		CH_4<2 ppm	CH_4<0.5 ppm	He,Xe<1 ppm	H_2,Ne<1 ppm
				THC<3 ppm	

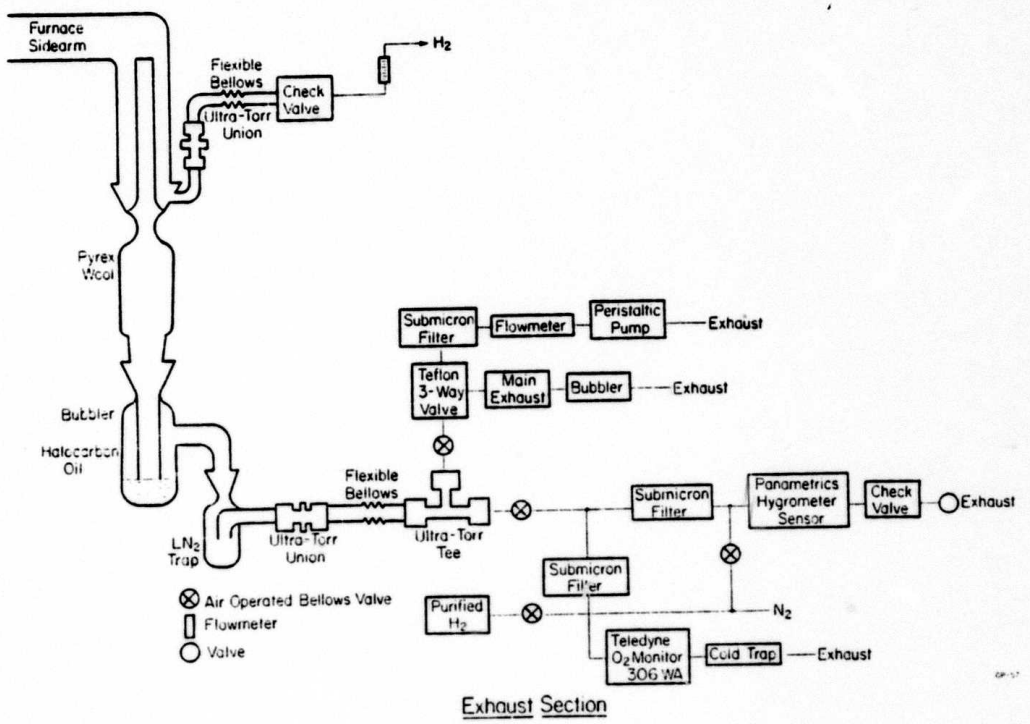

Figure 19. Exhaust system schematic.

exhaust trap was replaced with high temperature Apiezon H grease which is good up to 250°C (compared to 100°C for the Halocarbon grease.) A fan is used for additional cooling of this joint and thus it is possible to keep the heating tape very hot without affecting this seal.

The peristaltic pump, which is used during the loading of a substrate into the system, is separated from the main exhaust line by a 3-way teflon valve in order to prevent contamination of this section. The peristaltic pump uses gum rubber tubing and constant exposure to the main exhaust products would greatly shorten its lifetime. A teflon valve was used instead of a stainless steel valve because of the reactivity of the exhaust products with stainless steel. The non-sticking nature of the teflon surface insures that the valve will not become plugged.

A high sensitivity O_2 monitor which can detect as small a concentration as 0.02 ppm O_2 and a Panametrics hygrometer sensor are also connected to the main exhaust line. They can be used to evaluate the leak integrity of the system as a whole and also serve as a calibration tool for the addition of O_2 to the main gas stream. Unfortunately, these instruments can not be used during an actual growth run as the exhaust products would cause their demise in a relatively short period of time.

The main furnace tube has also been modified. The double O-Ring stainless steel joints which formed the seal on top of the indium and gallium source arms and the dead space between these joints and the taper joints on the source boats were eliminated. The top seals (between the source boat and the individual source arms) are now made with a double O-Ring tapered quartz joint which is attached to the source boats. A quartz O-Ring ball joint forms the seal on top of the source boat. This arrangement greatly reduces the amount of time that it takes to load the source materials into the boats.

The water jackets which were used to keep the upper O-Ring joints cool were removed and cooling is now done with two fans.

Other changes in the main tube included the addition of a baffle in the mixing zone region to aid in the mixing of all the gases in order to promote homogeneity in composition for ternary and quaternary compounds and permanently sealing in the dump tube just below the exhaust sidearm. The deposits on the dump tube could easily be etched off with HCl without removing the tube. A removable liner was found to be a problem when working with the phosphorous compounds because of the pyrophoric nature of phosphorus.

F. $In_xGa_{1-x}As$ GROWTH

Growth of the ternary $In_xGa_{1-x}As$ on InP was initiated after the automated system was assembled. The composition of the ternary is strongly affected by the ratio of HCl (Indium)/HCl(Gallium) and this ratio was chosen to be 7. A growth temperature of 700°C was used for all initial growth runs.

The first run was successful and produced an 11 μm thick $In_xGa_{1-x}As$ layer that had a $\Delta a/a$ [(a(layer) - a(substrate))/a(substrate)] = 0.49% as determined by single crystal x-ray diffraction measurements. Assuming that the relationship between the amount of indium incorporated into the ternary alloy and the ratio of HCl(In)/HCl(Ga) is linear as it is for InGaAs/GaAs, the HCl(In)/ HCl(Ga) ratio of 6 was set to obtain a lattice match. A III-V ratio of 1.16 was used. This produced a lattice-matched layer but the x-ray diffraction peaks were broad (full width at half maximum 900 sec) indicating poor crystallinity or inhomogeneity in the grown layer. By comparison an InP substrate shows a typical FWHM of 200 sec, using the (400) reflection. With the HCl(In)/HCl(Ga) ratio held constant the HCl flow rates were doubled in order to put more indium and gallium into the system to see

if the broad x-ray diffraction widths might have been caused by vacancies. The III-V ratio was thus changed to 2.33. The layer remained lattice-matched but the x-ray peaks were unchanged. The growth rate also dropped by almost a factor of 4. With the growth conditions used for sample #2 but with the sample rotated during growth there was still no change in the x-ray line width indicating that the problem was not lateral inhomogeneity. An experiment was carried out to determine if thermal shock during growth initiation could be causing the broadening. For the initial runs the substrate was kept at about 500°C in the preheat zone. Since the stepper motor moves the sample from the preheat zone to its growth position in about 30 seconds it is quite possible that the sample does not have enough time to equilibrate to the growth temperature of 700°C.

The preheat temperature was adjusted to 700°C but the substrate was held at this temperature for only 5 minutes to minimize any chance of thermal damage. All other growth parameters were kept constant. The resulting growth was polycrystalline. Using the same flow rates and temperatures the next sample was kept in the preheat zone for 30 minutes. This time the sample was crystalline but displayed a mismatch of +0.81% which occurred because the previous two stage indium boat had been replaced by a three stage boat that was more efficient at transporting InCl than the two stage. This result implies that the lattice match should occur for a HCl(In)/HCl(Ga) ratio of 5 which is quite low compared to the published results of Varian.[49] Also of interest is the fact that the full width at half maximum decreased to 620 seconds. Thus, this would indicate that thermal shock was indeed part of the crystallinity problem.

There are many possible reasons why the grown ternary layers could be inhomogeneous. A major problem cited by RCA is inadequate mixing of the two chloride streams with AsH_3 and/or PH_3. They noted during their growth

studies of $In_xGa_{1-x}P$ that the x-ray line width depended upon how well the gas streams were mixed.[95] Another problem which can lead to poor crystal quality is not saturating the indium source with InCl. This will cause compositional grading at the substrate interface. It is also possible that inhomogeneity in the epitaxial layer can be caused by fluctuations in the gas flow rates.[51] The effect of any surface oxides on crystal quality is also unknown. Finally, it should be pointed out that the use of AsH_3 to prevent thermal damage to InP substrates was investigated. The use of AsH_3 instead of PH_3 is of interest because one would not have to worry about the troublesome phosphorous deposits in the exhaust and on the furnace tube. It is possible that by using the AsH_3 a layer of $InAs_xP_{1-x}$ may have been forming on the surface before growth and cause the x-ray line broadening.

Considering all the possible causes of x-ray line broadening it seemed likely that the cause was improper mixing. Thus another set of baffles were designed and sealed into the furnace tube. No change was noticed. A higher growth temperature (730°C) was tried to see if that might improve the line width. The line width stayed the same. The use of PH_3 instead of AsH_3 in the preheat zone before growth also did not decrease the line width.

Since thermal shock was found to affect the line width before, it was decided to investigate the preheat treatment more thoroughly. Instead of raising the sample directly from the base of the furnace tube to its position in the preheat zone in one step, the sample was raised 2 inches at a time and allowed to equilibrate 10 minutes at each step. This permitted the growth of epitaxial $In_xGa_{1-x}As/InP$ layers with line widths of 450".

Now that this major problem of x-ray line width broadening has been solved the growth parameters and material characteristics of $In_xGa_{1-x}As$ and

$In_xGa_{1-x}As_yP_{1-y}$ epitaxial layers will be thoroughly studied and the use of these materials in photodetectors for fiber communication systems will be investigated. Table 4 illustrates the best results obtained with the two systems.

TABLE 4

Highest Purity Results

Material	n(300°K) cm^{-3}	μ(300°K) $cm^2/V-s$	n(77°K) cm^{-3}	μ(77°K) $cm^2/V-s$
GaAs	2.1×10^{14}	6810	3×10^{14}	75,670
GaAs	4×10^{14}	5082	3.4×10^{14}	72,332
GaAs	1.1×10^{15}	4645	8.3×10^{14}	73,561
InP	2.3×10^{14}	2750	1.7×10^{14}	29,750
InP	2.3×10^{15}	2600	1.1×10^{15}	28,404
$In_xGa_{1-x}As/InP$	6.8×10^{15}	5840	3.2×10^{15}	6,310
$In_xGa_{1-x}As/InP$	6.3×10^{15}	6780	4.4×10^{15}	18,170

V. REFERENCES

1. N. Holonyak, Jr., R.M. Kolbas, R.D. Dupuis, and P.D. Dapkus, "Quantum-well heterostructure lasers," IEEE J. Quantum Electron., vol. QE-16, pp. 170-186, Feb 1980.

2. E.A. Rezek, N. Holonyak, Jr., B.A. Vojak, G.E. Stillman, J.A. Rossi, D.L. Keune, and J.D. Fairing, "LPE $In_{1-x}Ga_xP_{1-z}As_z$ (x~0.12, z~0.26) DH laser with multiple thin-layer (<500 Å) active region," Appl. Phys. Lett., vol. 31, pp. 288-290, Aug. 15, 1977.

3. E.A. Rezek, H. Shichijo, V.A. Vojak, and N. Holonyak, Jr., "Confined-carrier luminescence of a thin $In_{1-x}Ga_xP_{1-z}As_z$ well (x~0.13, z~0.29; ~400 Å) in an InP p-n junctions," Appl. Phys. Lett., vol. 31, pp. 534-536, Oct. 15, 1977.

4. E.A. Rezek, N. Holonyak, Jr., B.A. Vojak, and H. Shichijo. "Tunnel injection into the confined-particle states of an $In_{1-x}Ga_xP_{1-z}As_z$ well in InP," Appl. Phys. Lett., vol. 31, pp. 703-795, Nov. 15, 1977.

5. E.A. Rezek, N. Holonyak, Jr., B.A. Vojak, and H. Shichijo, "Single and multiple thin layer (L_z<400 Å) $In_{1-x}Ga_xP_{1-z}As_z$-InP heterostructure light emitters and lasers (λ~1.1 μm, 77°K)," J. Appl. Phys., vol. 49, pp. 69-74, Jan. 1978.

6. E.A. Rezek, B.A. Vojak, and N. Holonyak, Jr., "Bandfilling in liquid phase epitaxial InP-$In_{1-x}Ga_xP_{1-z}As_z$-InP quantum-well heterostructure lasers," J. Appl. Phys., vol. 49, pp. 5398-5403, Nov. 1978.

7. R. Chin, N. Holonyak, Jr., S.W. Kirchoefer, R.M. Kolbas, and E.A. Rezek, "Determination of the valence-band discontinuity of InP-$In_{1-x}Ga_xP_{1-z}As_z$ (x~0.13, z~0.29) by quantum-well luminescence," Appl. Phys. Lett., vol. 34, pp. 862-864, June 15, 1979.

8. E.A. Rezek, R. Chin, N. Holonyak, Jr., S.W. Kirchoefer, and R.M. Kolbas, "Phonon-assisted recombination in a multiple quantum-well LPE InP-$In_{1-x}Ga_xP_{1-z}As_z$ heterostructure laser," Appl. Phys. Lett., vol. 35, pp. 45-47, July 1, 1979.

9. E.A. Rezek, R. Chin, N. Holonyak, Jr., S.W. Kirchoefer, and R.M. Kolbas, "Quantum-well InP-$In_{1-x}Ga_xP_{1-z}As_z$ heterostructure lasers grown by liquid phase epitaxy (LPE)," Electron. Mater. Conf., Boulder, CO, June 1979, J. Electron. Mater., vol. 9, pp. 1-27, Jan. 1980.

10. E.A. Rezek, N. Holonyak, Jr., and B. Fuller, "Temperature dependence of threshold current for coupled multiple quantum-well $In_{1-x}Ga_xP_{1-z}As_z$-InP heterostructure laser diodes," J. Appl. Phys., vol. 51, to be published, May, 1980.

11. E.A. Rezek, B.A. Vojak, R. Chin, and N. Holonyak, Jr., "Compositional inhomogeneity of liquid phase epitaxial InGaPAs layers observed directly in photoluminescence," Appl. Phys. Lett., vol. 36, pp. 744-746, May 1, 1980.

12. E.A. Rezek, B.A. Vojak, R. Chin, N. Holonyak, Jr., and E.A. Sammann, "Thin-layer liquid phase epitaxy of InGaPAs heterostructures in short intervals (<100ms): non-diffusion-limited crystal growth," Electronic Materials Conference, June, 1980, Ithaca, J. Electronic Materials, to be published.

13. M. Feng, M. M. Tashima, T. H. Windhorn, and G. E. Stillman "Composition dependence of the influence of lattice mismatch on surface morphology in LPE growth of InGaAsP on (100)-InP," Apply. Phys. Lett., vol. 33, pp. 533-536, Sept. 1978.

14. M. Feng, L. W. Cook, M. M. Tashima, and G. E. Stillman, "Auger profile study of the influence of lattice mismatch on the LPE InGaAsP-InP heterojunction interface," Appl. Phys. Lett., vol. 34, pp. 697-699, May 1979.

15. L. W. Cook, M. Feng, M. M. Tashima, R. J. Blattner, and G. E. Stillman, "Interface grading in InGaAsP liquid phase epitaxial heterostructures," to be published in Appl. Phys. Lett., July 1980.

16. M. Feng, M. M. Tashima, L. W. Cook, R. A. Milano, and G. E. Stillman, "The influence of growth-solution dopants on distribution coefficients in the LPE growth of InGaAsP," Appl. Phys. Lett., Vol. 34, pp. 91-93, Jan. 1979.

17. M. Feng, M. M. Tashima, L. W. Cook, and C. E. Stillman, "Impurity dependence of distribution coefficients in the LPE growth of InGaAsP," Proceedings of the Symposium on Gallium Arsenide and Related Compounds, St. Louis, 1978, Inst. Phys. Conf. Ser. 45 (Institute of Physics and Physical Society, London, 1979), pp. 61-70.

18. M. Feng, L. W. Cook, M. M. Tashima, T. H. Windhorn, and G. E. Stillman, "The influence of LPE growth techniques on the alloy composition of InGaAsP," Appl. Phys. Lett. vol. 34, pp. 292-295, Feb. 1979.

19. M. Feng, L. W. Cook, M. M. Tashima, and G. E. Stillman, "Lattice constant, band gap, thickness, and surface morphology of InGaAsP-InP layers grown by step-cooling, equilibirum-cooling, supercooling and two-phase-solution growth techniques," Electronic Materials Conference, June, 1978, Boulder, CO, J. Electronic Materials, vol. 9, No. 2, pp. 241-280, 1980.

20. L. W. Cook, M. M. Tashima, and G. E. Stillman, "Effects of a finite melt on the thickness and composition of liquid phase epitaxial InGaAsP and InGaAs layers grown by the diffusion-limited step-cooling technique," Appl. Phys. Lett., vol. 36, pp. 904-907, June 1980.

21. M. Feng, J. D. Oberstar, T. H. Windhorn, L. W. Cook, G. E. Stillman, and B. G. Streetman, "Be-implanted 1.3 μm InGaAsP avalanche photodetectors," Appl. Phys. Lett., vol. 34, pp. 591-593, May 1979.

22. G. B. Stringfellow and H. T. Hall, "VPE Growth of $Al_xGa_{1-x}As$," J. of Crystal Growth, vol. 43, pp. 47-60, 1978.

23. G. B. Stringfellow, "VPE Growth of III/V Semiconductors," Annual Review of Material Science, vol. 8, pp. 73-98, 1978.

24. B. E. Barry, "Vapor Phase Growth of Semiconducting Layers," Thin Solid Films, vol. 39, pp. 35-53, 1976.

25. H. M. Manasevit and W. I. Simpson, "The Use of Metal-Organics in the Preparation of Semiconductor Materials, I. Epitaxial Gallium - V. Compounds," J. Electrochemical Soc., vol. 116, pp. 1725-1732 (1969).

26. H. M. Manasevit and W. I. Simpson, "The Use of Metalorganics in the Preparation of Semiconductor Materials, V. The Formation of In-Group V Compounds and Alloys," J. Electrochemical Soc., vol. 120, pp. 135-137, 1973).

27. J. P. Duchemin, M. Bonnet, G. Beuchet, and F. Koelsch, "Organometallic Growth of Device-Quality InP by Cracking of $In(C_2H_5)_3$ and PH_3 at Low Pressure," Proc. of the Symposium on Gallium Arsenide and Related Compounds (St. Louis) (Inst. of Physics, Conf. Series No. 45 Bristol and London) pp. 10-18, 1978.

28. H. Renz, J. Weidlein, K. Benz, and M. Pilkuhn, "InP Epitaxy with a New Metalorganic Compound," Electronics Letters, vol. 16, p. 228, March 13, 1980.

29. M. J. Tsai and R. H. Bube, "Electrical Properties of n-Type Epitaxial Indium Phosphide Films," J. Appl. Phys., vol. 49, pp. 3397-3401, June 1978.

30. C. B. Cooper III, M. J. Ludowise, V. Aebi, and R. L. Moon, "Use of Trimethylantimony and Trimethylarsenic for Organometallic V.P.E. Growth of $GaAs_{1-y}Sb_y$ and $Ga_{1-x}In_xAs$," Electronics Letters, vol. 16, pp. 20-21, January 3, 1980.

31. B. Baliga and S. Ghandi, "Growth and Properties of Heteroepitaxial GaInAs Alloys on GaAs Substrates Using Trimethylgallium, Triethylindium, and Arsine," J. Electrochemical Society, vol. 122, pp. 683-687, May 1975.

32. J. P. Noad and A. J. SpringThorpe, "The Preparation of $Ga_{1-x}In_xAs$ by Organometallic Pyrolysis for Homojunction LED's," J. Electronic Materials, vol. 9, pp. 601-620, May 1980.

33. C. Cooper III, M. J. Ludowise, V. Aebi, and R. L. Moon, "The Organometallic VPE Growth of $GaAs_{1-y}Sb_y$ Using Trimethylantimony and $Ga_{1-x}In_xAs$ Using Trimethylarsenic," J. Electronic Materials, vol. 9, pp. 299-309, 1980.

34. J. Hirtz, J. P. Duchemin, P. Hirtz, B. deCremoux, T. Pearsall, and M. Bonnet, "$Ga_xIn_{1-x}As_vP_{1-v}$/InP D.H. Laser Emitting at 1.15 μm Grown by Low-Pressure Metalorganic C.V.D.," Electronics Letters, vol. 16, pp. 275-277, April 10, 1980.

35. J. R. Knight, D. Effer, and P. R. Evans, "The Preparation of High Purity Gallium Arsenide by Vapour Phase Epitaxial Growth," Solid State Electronics, vol. 8, pp. 178-180, 1965.

36. C. M. Wolfe and G. E. Stillman, "High Purity GaAs," Proc. of the Symposium on Gallium Arsenide and Related Compounds (Aachen) (Inst. of Physics, Conf. Series No. 9, Bristol and London) pp. 3-17, 1970.

37. J. DiLorenzo, "Vapor Growth of Epitaxial GaAs: A Summary of Parameters Which Influence the Purity and Morphology of Epitaxial Layers," Journal of Crystal Growth, vol. 17, pp. 189-206, 1972.

38. R. C. Clarke and L. L. Taylor, "Pure and Doped Indium Phosphide by Vapour Phase Epitaxy," Journal of Crystal Growth, Vol. 43, pp. 473-479, 1978.

39. R. C. Clarke, B. D. Joyce, and W.H.E. Wilgoss, "The Preparation of High Purity Epitaxial InP," Solid State Communications, vol. 8, pp. 1125-1128, 1970.

40. B. D. Joyce and E. W. Williams, "The Preparation and Photoluminescent Properties of High Purity Vapour Grown Indium Phosphide Layers," Proc. of the Symposium on Gallium Asenide and Related Compounds (Aacken) (Inst. of Physics, Conf. Series, No. 9, Bristol and London), pp. 57-63, 1970.

41. R. D. Fairman, M. Omori, and F. B. Fank, "Recent Progress in the Control of High Purity VPE InP by the $PCl_3/In/H_2$ Technique," Proc. of the Symposium on Gallium Arsenide and Related Compounds (St. Louis) (Inst. of Physics, Conf. Series No. 33b, Bristol and London), pp. 45-54, 1976.

42. C. M. Wolfe, G. E. Stillman, and I. Melngailis, "Epitaxial Growth of $In_xGa_{1-x}As$ Waveguide Detectors for Integrated Optics," J. Electrochemical Society, vol. 121, pp. 1506-1509, November 1974.

43. A. Humbert, "Study of the Growth of Epitaxial Layers and its Application to (Ga,In) As Composites," Philips Res. Repts. vol. 31, pp. 216-243, 1976.

44. S. Hyder, "Thin Film Epitaxial Growth of $In_xGa_{1-x}As$ on GaAs," J. Electrochemical Society, vol. 123, pp. 1503-1508, October 1976 .

45. J. J. Tietjen and J. A. Amick, "The Preparation and Properties of Vapor Deposited Epitaxial $GaAs_{1-x}P_x$ Using Arsine and Phosphine," J. Electrochemical Society, vol. 113, pp. 724-728, 1966.

46. K. Ahmad and A. Mabbitt, "Gallium Indium Arsenide Photodiodes," Solid State Electronics, vol. 22, pp. 327-333, 1979.

47. N. Susa, Y. Yamauchi, and H. Kaube, "Punch-Through Type InGaAs Photodetector Fabricated by Vapor Phase Epitaxy," IEEE Journal of Quantum Electronics, vol. QE-16, pp. 542-545, May 1980.

48. G. Olsen, C. Nuese, and M. Ettenberg, "Reliability of Vapor-Grown InGaAs and InGaAsP Heterojunction Laser Structures," IEEE Journal of Quantum Electronics, vol. QE-15, pp. 688-693, August 1979.

49. S. B. Hyder, R. R. Saxena, S. H. Chiao, and R. Yeats, "Vapor-Phase Epitaxial Growth of InGaAs Lattice Matched to (100) InP for Photodiode Application," Appl. Phys. Lett., vol. 35, pp. 787-789, November 15, 1979.

50. N. Susa, Y. Yamauchi, H. Ando, and H. Kaube, "Planar Type Vapor-Phase Epitaxial $In_{0.53}Ga_{0.47}As$ Photodiode," IEEE Electron Device Letters, vol. EDL-1, pp. 55-57, April 1980.

51. N. Susa, Y. Yamauchi, H. Ando, and H. Kaube, "Vapor-Phase Epitaxial Growth of InGaAs on (100) InP Substrate," Japanese Journal of Applied Physics, vol. 19, pp. L17-L20, January 1980.

52. H. Kaube, Y. Yamauchi and N. Susa, "Vapor-Phase Epitaxial $In_xGa_{1-x}As$ on (100), (111) A, and (111) B InP substrates," Appl. Phys. Lett., vol. 35, pp. 603-605, October 15, 1979.

53. K. Sugiyama, H. Kojima, H. Enda, and M. Shibata, "Vapor Phase Epitaxial Growth and Characterization of $Ga_{1-y}In_yAs_{1-x}P_x$ Quaternary Alloys," Japanese Journal of Applied Physics, vol. 16, pp. 2197-2203, December 1977.

54. S. B. Hyder, R. R. Sazena, and C. C. Hooper, "Vapor-Phase Epitaxial Growth of Quaternary $In_{1-x}Ga_xAs_yP_{1-y}$ in the 0.75 - 1.35 eV Band-Gap Range," Appl. Phys. Lett., vol. 34, pp. 584-586, May 1, 1979.

55. G. Olsen and H. Kressel, "Vapour Grown 1.3 μm InGaAsP/InP Avalanche Photodiodes," Electronics Letters, vol. 15, pp. 141-142, March 1, 1979.

56. G. Olsen, C. Nuese, and M. Ettenberg, "Low-threshold 1.25 μm Vapor-Grown InGaAsP cw lasers," Applied Physics Letters, vol. 34, pp. 262-264, February 15, 1979.

57. T. Mizutani, M. Yoshida, A. Usui, H. Watanabe, T. Yuasa, and I. Hayashi, "Vapor Phase Growth of InGaAsP/InP DH Structures by the Dual-Growth-Chamber Method," Japanese Journal of Applied Physics, vol. 19, pp. L113-L116, February 1980.

58. E. Enda, "Preparation and Properties of Vapor-Phase-Epitaxial-Grown GaInAsP," Japanese Journal of Applied Physics, vol. 18, pp. 2167-2168, 1979.

59. G. H. Olsen and T. J. Zamerowski, "Crystal Growth and Properties of Binary, Ternary, and Quaternary (In, Ga) (As, P) Alloys Grown by the Hydride Vapor Phase Epitaxy Technique," Progress in Crystal Growth and Characterization, vol. 2, pp. 309-375, 1979.

60. R. E. Enstrom, D. Richman, M. S. Abrahams, J. R. Appert, D. G. Fisher, A. H. Sommer, and B. F. Williams, "Vapour Growth of $Ga_{1-x}In_xAs$ Alloys for Infrared Photocathode Applications," Proceedings of the Symposium on Gallium Arsenide and Related Compounds (Aachen) (Inst. of Physics, Conf. Series No. 9, Bristol and London), pp. 30-40, 1970.

61. C. J. Nuese, D. Richman, and R. B. Clough, "The Preparation and Properties of Vapor-Grown $In_{1-x}Ga_xP$," Metallurgical Transactions, vol. 2, pp. 789-794, March 1971.

62. R. E. Enstrom, C. J. Nuese, V. S. Ban, and J. R. Appert, "Influence of Gas Phase Stoichiometry on the Properties of Vapour-Grown $In_{1-x}Ga_xP$ alloys," Proceedings of the Symposium on Gallium Arsenide and Related Compounds (Boulder) (Inst. of Physics, Conf. Series No. 17, Bristol and London), pp. 37-47, 1972.

63. V. Ban, "Mass Spectrometric and Thermodynamic Studies of the CVD of Some III-V Compounds," J. Crystal Growth, vol. 17, pp. 19-23, 1972.

64. C. O. Bozler, "Gallium Arsenide Vapor Epitaxy," Solid State Research (Lincoln Laboratory) #2, pp. 52-53, 1975.

65. C. O. Bozler, J.C.C. Fan, and R. W. McClelland, "Efficient GaAs Shallow-Homojunction Solar Cells on Ge Substrates," Proceedings of the Symposium on Gallium Arsenide and Related Compounds (St. Louis) (Inst. of Physics, Conf. Series No. 45, Bristol and London), pp. 429-436, 1978.

66. D. Effer, "Epitaxial Growth of Doped and Pure GaAs in an Open Flow System," Journal of the Electrochemical Society, vol. 112, pp. 1020-1025, October 1965.

67. C. M. Wolfe, A. G. Foyt, and W. T. Lindley, "Epitaxial Gallium Arsenide for High-Efficiency Gunn Oscillators," Electrochemical Technology, vol. 6, pp. 208-214, May-June 1968.

68. R. E. Enstrom and J. R. Appert, "Vapour-phase Growth of Large-Area Microplasma-free p-n junctions in GaAs and $GaAs_{1-x}P_x$," Proceedings of the Symposium on Gallium Arsenide and Related Compounds (Dallas) (Inst. of Physics, Conf. Series No. 7, Bristol and London) pp. 213-221, 1968.

69. L. C. Bobb, H. Holloway, K. H. Maxwell, and E. Zimmerman, "Oriented Growth of Semiconductors - II Homoepitaxy of Gallium Arsenide," Journal of Physics and Chemistry of Solids, vol. 27, pp. 1679-1685, 1966.

70. B. Cairns and R. Fairman, "Effects of the $AsCl_3$ Concentration on Electrical Properties and Growth Rates of Vapor Grown Epitaxial GaAs," Journal of the Electrochemical Society, vol. 115, p. 327C, 1968.

71. B. Cairns and R. Fairman, "Effect of the $AsCl_3$ Concentration on Impurity Incorporation in Vapor Grown Epitaxial GaAs," Journal of the Electrochemical Society, vol. 117, p. 197C, 1970.

72. J. V. DiLorenzo, G. E. Moore, Jr., and A. E. Machala, "Dependence of the Electrical Properties of Vapor Grown Epitaxial GaAs on the $AsCl_3$ Vapor Concentration," Journal of the Electrochemical Society, vol. 117, p. 102C, 1970.

73. J. V. DiLorenzo and G. E. Moore, "Effects of the $AsCl_3$ Mole Fraction on the Incorporation of Germanium, Silicon, Selenium, and Sulfur into Vapor Grown Epitaxial Layers on GaAs," Journal of the Electrochemical Society, vol. 118, pp. 1823-1830, November 1971.

74. J. K. Kennedy, W. D. Potter, and D. E. Davis, "The Effect of the Hydrogen Carrier Gas Flow Rate on the Electrical Properties of Epitaxial GaAs Prepared in a Hydride System," Journal of Crystal Growth, vol. 24/25, pp. 233-238, 1974.

75. H. B. Pogge and B. M. Kemlage, "Doping Behavior of Silicon in Vapor-Grown III-V Epitaxial Films," Journal of Crystal Growth, vol. 31, pp. 183-189, 1975.

76. R. C. Clarke and L. L. Taylor, "Multilayered Structures of Epitaxial Indium Phosphide," Journal of Crystal Growth, vol. 31, pp. 190-196, 1975.

77. J. V. DiLorenzo and A. E. Machala, "Orientation Effects on the Electrical Properties of High Purity Epitaxial GaAs," Journal of Electrochemical Society, vol. 118, pp. 1516-1517, September 1971.

78. M. C. Hales, "Kinetics of the Vapour Phase Deposition of Epitaxial InP," Journal of Electronic Materials, vol. 9, pp. 355-370, March 1980.

79. Tatsuo Aoki, "High Purity Epitaxial GaAs," Japanese Journal of Applied Physics, vol. 14, pp. 1267-1271, September 1975.

80. B. E. Barry, "Optimization of Growth Conditions to Produce High Purity Epitaxial Gallium Arsenide for Gunn Devices," Proceedings of the Symposium on Gallium Arsenide and Related Compounds, (Aachen) (Inst. of Physics, Conf. Series No. 9, Bristol and London) pp. 172-183, 1970.

81. M. E. Weiner, "Si Contamination in Open Flow Quartz Systems for the Growth of GaAs and GaP, Journal of the Electrochemical Society, vol. 119, pp. 496-504, April 1972.

82. M. Ettenberg, G. H. Olsen, and C. J. Nuese, "Effect of Gas-Phase Stoichiometry on the Minority-Carrier Diffusion Length in Vapor-Grown GaAs," Applied Physics Letters, vol. 29, pp. 141-142, August 1976.

83. M. S. Abrahams and C. J. Buiocchi, "Twins and Stacking Faults in Vapor Grown GaAs," Journal of Physics and Chemistry of Solids, vol. 28, pp. 927-930, 1967.

84. S. R. Bhola and A. Mayer, "Epitaxial Deposition of Silicon by Thermal Decomposition of Silane," RCA Review, vol. 24, pp. 511-522, December 1963.

85. S. Mendelson, "Stacking Fault Nucleation in Epitaxial Silicon on Variously Oriented Silicon Substrates," Journal of Applied Physics, vol. 35, pp. 1570-1581, May 1964.

86. Y. Nonomura, Y. Okuno, and J. Nishizawa, "Surface Morphology of GaAs Grown by Vapor Phase Epitaxy," Journal of Crystal Growth, vol. 46, pp. 795-800, 1979.

87. A. R. Clawson, D. A. Collins, D. I. Elder, and J. J. Monroe, "Laboratory Procedures for Etching and Polishing InP Semiconductor," N.O.S.C. Technical Note 592, 1978.

88. V. S. Ban and M. Ettenberg, "Mass Spectrometric and Thermodynamic Studies of Vapor-Phase Growth of $In_{1-x}Ga_xP$," Journal of Physics and Chemistry of Solids, vol. 34, pp. 1119-1129, 1973.

89. D. L. Rode, "Electron Transport in InSb, InAs, and InP," Physical Review B, vol. 3, pp. 3287-3299, May 15, 1971.

90. H. Bruch, L. Palm, F. Ponse, and P. Balk, "V.P.E. GaAs M.E.S.F.E.T. Structure Using Oxygen Injection During Buffer Layer Growth," Electronics Letters, vol. 15, pp. 246-247, April 26, 1979.

91. G. B. Stringfellow and G. Hom, "Hydride VPE Growth of GaAs for FET's," Journal of the Electrochemical Society, vol. 124, pp. 1806-1811, November 1977.

92. M. C. Hales and J. R. Knight, "The Electrical Properties of Vapour Epitaxial Indium Phosphide Grown in the Presence of Oxygen," Journal of Crystal Growth, vol. 46, pp. 582-584, 1979.

93. L. Palm, H. Bruch, K. H. Bachem, and P. Balk, "Effect of Oxygen Injection During VPE Growth of GaAs Films," Journal of Electronic Materials, vol. 8, pp. 555-570, September 1979.

94. G. B. Stringfellow, H. T. Hall, Jr., and R. A. Burmeister, "Electrical Properties of Nitrogen-Doped GaP," Journal of Applied Physics, vol. 46, pp. 3006-3011, July 1975.

95. A. G. Sigai, C. J. Nuese, R. E. Enstrom, and T. Zamerowski, "Vapor Growth of $In_{1-x}Ga_xP$ for p-n Junction Electroluminescence I. Material Preparation," Journal of the Electrochemical Society, vol. 120, pp. 947-955, July 1973.